Faculty of Civil Engineering and Geodesy
Chair for Computation in Engineering
Prof. Dr. rer. nat. Ernst Rank

Polyhedral Mesh Generation for CFD-Analysis of Complex Structures

Georgios Balafas

Master's thesis
for the Master of Science program
Computational Mechanics

Author: Georgios Balafas

Matriculation number: 03625427

Supervisors:

Prof. Dr.-Ing. Casimir Katz

Dr.-Ing. Stefan Kollmannsberger

Dr.-Ing. Andreas Niggl

Date of issue: 08 October 2014

Date of submission: 03 April 2014

Involved Organisations

Chair for Computation in Engineering
Faculty of Civil Engineering and Geodesy
Technische Universität München
Arcisstraße 21
D-80333 München

SOFiSTiK AG
Bruckmannring 38
D-85764 Oberschleißheim

Declaration

With this statement I declare, that I have independently completed this Master's thesis. The thoughts taken directly or indirectly from external sources are properly marked as such. This thesis was not previously submitted to another academic institution and has also not yet been published.

München, April 1, 2014

Georgios Balafas

Georgios Balafas
e-Mail: georg.balafas@tum.de

Acknowledgments

The present work forms the final act of my studies in the Master's Program Computational Mechanics, Technische Universität München, and is the outcome of several months of personal effort and dedication. However, it would not have been possible without the contribution of a number of people, to whom I feel the need to express my gratitude.

First and foremost, I would like to thank my supervisors for our excellent cooperation throughout my Master's Thesis. As their role has surpassed the typical duties in Academia, I have preferred to mention them in the chronological order that I have met each one of them, as I have been progressing with my education and life.

To begin with, Dr. Stefan Kollmannsberger (CiE – TUM), whose support has not been constrained merely within the scope of the present work, but has provided me with guidance since the beginning of my studies in TUM. More importantly, for believing in me and, with his sincere encouragement, for his mentoring on subjects that exceed the scope of Academic life.

Furthermore, Prof. Casimir Katz (SOFiSTiK AG / CiE – TUM) for trusting me with a demanding subject and being helpful in every possible way. With his thoughtful advice and large knowledge on a vast range of scientific topics, he has contributed to my work at crucial points of its progress. Furthermore, through him, I would like to thank the SOFiSTiK AG family, for making me feel welcome in every way.

And, of course, especially Dr. Andreas Niggl (SOFiSTiK AG), who has inspired me with his professionalism, knowledge and motivation, in order to accomplish

the goals of this Master's Thesis. I wouldn't neglect to mention how grateful I feel for his patience, as he has always been available and willing to answer my numerous questions and requests, with his enlightening point of view, guiding me closely through every step of this work.

Additionally, I would like to acknowledge the contribution of Mr. Henk Krüs, from Cyclone Fluid Dynamics BV, for his kind feedback regarding topics on CFD simulation and DOLFYN CFD analysis code, as well as Mr. Felix Frischmann for his insight into mesh generation topics.

Finally, I would like to express my warm feelings about all those people that have made my studies much more instructive and pleasant than I had ever imagined, as well as making me feel more than welcome in a completely new environment. A honorary mention, for this, is dedicated to the whole development team of AdhoC++ Finite Element code, of the Chair for Computation in Engineering, under the general supervision of Dr. Kollmannsberger. For more than two years, this team has been home of my educational, as well as professional, progress and achievements. To my direct supervisors and closest teammates, while working on this project, Mr. Nils Zander and Mr. Tino Bog, I owe my sincere appreciation.

Last but not least, there are no words to express my feelings about my friends and, especially, my family, who have been by my side for as long as my memory allows me to recall. Words will have to be kept outside these pages and be expressed in our own, personal way.

April 2014, München Georgios Balafas

Contents

Chapter 1

Introduction

1.1 Motivation

In many disciplines of engineering, simulation using Computational Fluid Dynamics (CFD) is of constantly increasing interest. With the continuously growing capabilities of modern computing systems, the demand for more detailed analysis and assessment of fluid behavior is growing as well. However, the flow domain is in most cases defined by complex geometries, for which it is not always easy to establish a high quality discretized model.

Whenever possible, analysts prefer the use of hexahedral meshes in 3D simulations, in a similar way that quadrilateral meshes are preferred for 2D analysis cases. This is supported by the fact that hexahedra, as well as quadrilaterals, present geometric properties that result to high quality meshes and desirable numerical behavior. However, while for 2D domains automatic quadrilateral mesh generation is generally possible, a corresponding robust method for arbitrary 3D domains is yet to come. The task of automatically generating well-conditioned, pure hexahedral meshes for complex geometries still remains open, even though significant progress has been made during the past decade [25, 12, 38, 15].

The answer to this challenge has, for many years, been the use of tetrahedra. They are the simplest form of volume elements, yet tetrahedral meshes are able to approximate any arbitrarily shaped continuum with a remarkable level of

detail. Automated tetrahedral mesh generation methods have been well studied and developed, providing currently the only robust solution for meshing complex geometries in 3D, making them a standard choice of major CFD codes.

However, despite the fact that tetrahedra present several geometric assets, such as planar faces and well defined face and volume centroids, they suffer from certain disadvantages that make analysts deem them inferior to hexahedra. Tetrahedral elements cannot provide reasonable accuracy, as soon as they become too elongated, which is often the case in boundary layers or sharp corners of the domain. Furthermore, they have only four neighbors (Fig. 1.1a), making them not an optimal choice for CFD, as computation of gradients at cell centers can become problematic. It is, therefore, not unusual during simulations serious numerical stability issues to appear, additionally to the reduced accuracy, and problematic convergence properties to dominate the analysis.

Several remedies exist, in order to overcome those disadvantages. A boundary layer, formed using prismatic elements along walls, is able to balance, up to a certain degree, the negative effects in accuracy and stability. Furthermore, advanced discretization methods combined with very fine meshes can result to accurate solutions and good convergence properties. This, however, demands for increased memory usage and computing time, while it makes the analysis code more complicated.

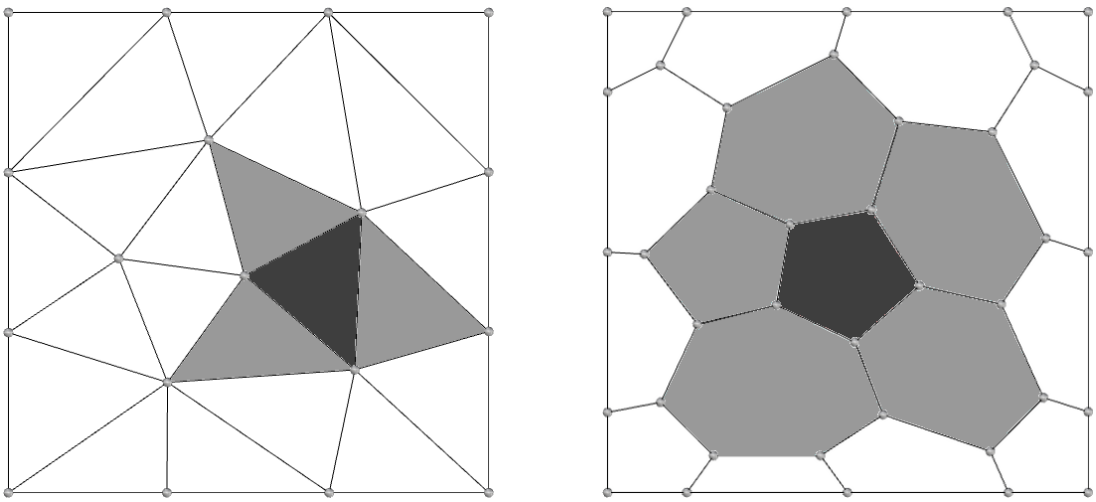

(a) Triangular element adjacencies **(b)** Polygonal element adjacencies

Figure 1.1: Neighboring elements for triangular and polygonal meshes

Recently, an alternative option to tetrahedral meshes has emerged, suggesting the use of polyhedral elements instead [22, 10]. Polyhedra offer the same level of automatic mesh generation as tetrahedra do, while they are able to overcome the disadvantages adherent to tetrahedral meshes. A major advantage of polyhedra occurs from the fact that they are bounded by many neighbors (Fig. 1.1b), making approximation of gradients much better that tetrahedra. Furthermore, they are much less sensitive to stretching and, since their typically irregular shape is not a restriction for several CFD codes, they offer the possibility of post-processing and optimization without the strict geometric criteria that are necessary for optimizing tetrahedral, or even hexahedral meshes.

On the negative side, polyhedra are usually of much more complex geometry than regular solids, and, depending on the generation method, it cannot always be guaranteed that they are convex, or, even more, that their faces are planar. The topology of polyhedral meshes is, typically, also complex, preventing the implementation of efficient and easy to maintain generation algorithms from being straightforward. As a further consequence, polyhedral meshes require a considerable amount of adjacency relations, in comparison to tetrahedral and hexahedral meshes, making them candidates for resource expensive solutions.

All the above set the basis for an interesting field of exploration in volume meshing. Previous studies on the subject have shown promising results, however polyhedral meshing is still far from becoming a standard practice in CFD simulations. Some explanations for this may be its limited adoption from analysis codes and the fact that polyhedra are not an appropriate solution for every type of analysis, preventing, thus, researches not interested in fluid simulations from being motivated in further investing on the topic. It should be mentioned that, currently, polyhedral meshes attract more attention in fields such as Computer Graphics and Medical Imaging, wherein 3D volume rendering is of specific interest. However, the few researches dedicated to exploring polyhedral mesh generation for CFD remain active, making constant progress towards more efficient methods and high quality meshes.

Herein, an overview of the current status of polyhedral mesh generation is attempted, presenting the achievements so far and what is to be expected in the near future. Additionally, an inquiry into polyhedral mesh generation methods has been made with the aid of a mesh generation code that was developed, within

the scope of this study. A presentation of the basic implementation principles that were followed is made, with the hope to motivate further development on the subject. Finally, the results of a set of elementary CFD simulations are discussed, which have been made possible with the use of DOLFYN CFD code [3] and SOFiSTiK FEA software [1], in order to assess the performance of the implemented mesh generator, as well as to obtain a first evaluation of the analysis characteristics of polyhedral meshes.

1.2 Basic Concepts

1.2.1 Voronoi Tessellations

In the past years, the main focus, regarding polyhedral mesh generation, has been placed on generating Voronoi tessellations. These are structures consisting of partitions that correspond to a set of generator points, such that every location within a subdivision is closer to its generator than to any other. Voronoi tessellations are unbounded, with outer partitions extending to infinity. However, for the purpose of mesh generation, partitions on the exterior are truncated by the domain's boundary, forming, this way, a general polyhedral mesh (Fig. 1.2) [37, 10].

Despite their simple concept, direct generation of 3D Voronoi meshes, to be used within numerical simulations, is not always straightforward. One way to retrieve a Voronoi mesh is by applying half-plane intersections, which is, however, computationally expensive, with a complexity of $O(n^2 \, log \, n)$ [4]. Another way is using Fortune's plane sweep algorithm, which, while of reduced complexity $O(n \, log \, n)$ [4], its implementation for 3D space is considered rather complicated [10]. Furthermore, an additional obstacle to overcome, which applies in every mesh generation algorithm, is considering topology in 3D space itself, even when, conceptually, a method is well defined. Currently, it cannot be claimed that an efficient direct polyhedral mesh generation method exists, or a robust enough to be used in CFD simulations.

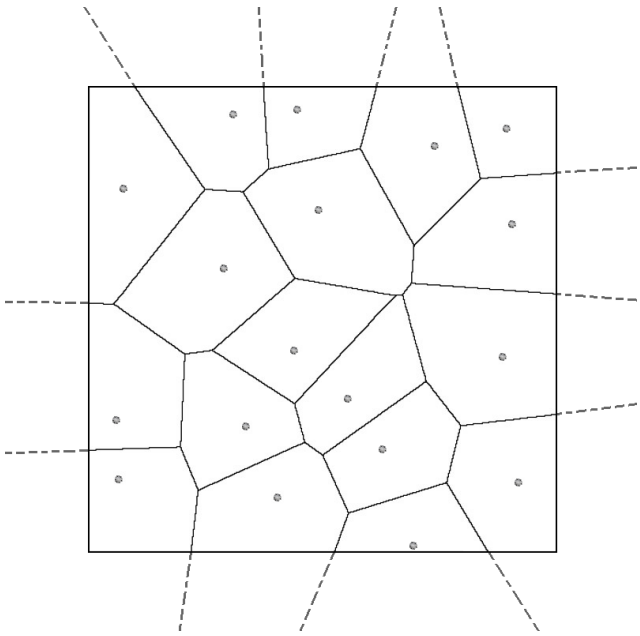

Figure 1.2: Bounded mesh formed by a Voronoi tessellation

1.2.2 Mesh Duality

A different approach in generating polyhedral meshes, which does not suffer by the aforementioned restrictions, comes with the introduction of indirect mesh generation methods. These are based on the principle of duality transforms, which define a mapping from entities of an input mesh, which is referred to as *primal*, to a destination mesh, referred to as *dual*. The main mapping process dictates that the vertices of a dual mesh are generated at the centers of the primal cells [17]. This relation is unique, leading to a one-to-one correspondence of the two counterpart meshes, while it is also characterized by inverse applicability. This means that the original primal mesh can be obtained back, if the same mapping is applied to the dual mesh.

This property can be applied for Voronoi tessellations, as well. The dual counterpart of a Voronoi mesh is a Delaunay triangulation, which is defined as a partitioning scheme, such that no vertex is inside the circumcircle of any triangle (Fig. 1.3). The implementation of Delaunay triangulation algorithms is relatively simple and can be of complexity $O(n\,log\,n)$, following Ruppert's algorithm [11]. As the duality property can be applied both ways, it is then possible to obtain a Voronoi mesh, by applying a duality transform on a previously generated

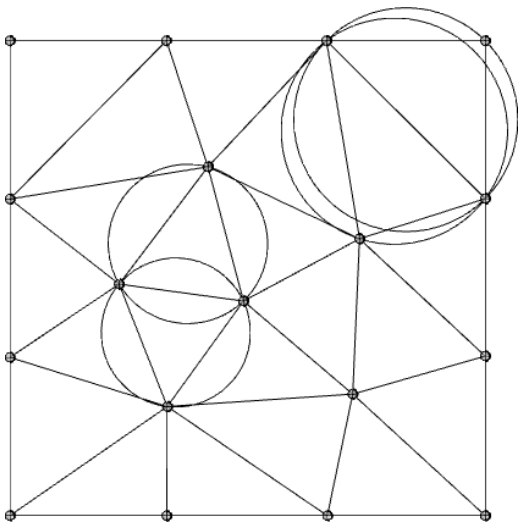

Figure 1.3: Mesh formed by a Delaunay triangulation

Delaunay triangulation, considering the circumcenters of the primal tetrahedra as generator vertices.

In 3D space, an equivalent mesh generation method would require a tetrahedral primal mesh that complies with the Delaunay criterion. Delaunay partitioning is known to maximize the minimum angle of all formed simplices, which leads to well conditioned tetrahedra. However, in order to obtain a valid dual mesh, a far stricter criterion needs to be fulfilled: that of well centered tetrahedra, meaning that the circumcenter of a primal cell needs to be located within its volume [10]. This is something that is not always possible, as tetrahedra at the boundaries may be very flat, having their circumcenters outside the model's domain, while the Delaunay criterion still remains fulfilled. Situations like this are especially encountered at sharp concavities of the geometric model, and several suggestions have been made in order to overcome this issue.

Extending the previous concepts, it should be noted that, even though Voronoi meshes are characterized by desirable numerical properties, a valid polyhedral mesh does not necessarily have to be one. Except for the boundaries, where cells are "forced" to conform to the model's geometry, non Voronoi polyhedra may exist in the interior as well. Hence, duality transforms do not have to be restricted to using exclusively primal meshes that are based on the Delaunay criterion. Other possibilities include non-Delaunay tetrahedral meshes, hexahedral or even mixed meshes, which are further discussed in chapter (Ch. 3).

Finally, the advantage of indirect mesh generation lies in the fact that efficient algorithms can be implemented in order to obtain topologically involved dual meshes, based on primal meshes with simple topology. Furthermore, the primal meshes, themselves, can be created following equally efficient and well-studied algorithms. This approach leads into an effective two-step mesh generation, rather than an expensive, direct one.

1.3 Previous Work

Numerous studies and implementations for the generation of Voronoi tessellations in 2D exist. However, when it comes to 3D, these are limited and the product of most cannot be guaranteed to be usable as a mesh for CFD simulations. The main reason for this emerges by the fact that many researchers focus on other fields of application, of which most notable is that of Computer Graphics. It is, nonetheless, worth mentioning some of them, not only for the sake of completeness, but mostly because the have been studied as a first step towards polyhedral meshing for simulations in engineering.

Qhull [24] Voronoi mesh generator has been used for many years to produce high quality 3D tessellations. However, its lack of support for non-convex domains make it difficult to use for structures of complex geometry. On the other hand, Voro++ [36], despite its flexibility in generating Voronoi partitions around generator points, it does not guarantee a fully connected mesh. Finally, Tetgen mesh generator [31] produces boundary conforming Voronoi partitions as duals of Delaunay tetrahedral meshes, however the issue of strictly conforming to sharp concavities seems, so far, not to be treated properly.

All the previous have been open source projects which focus primarily on computational geometry concepts. Regarding more engineering oriented implementations, OpenFOAM [20] is an open source CFD software package that has evolved to a multi-physics tool suitable for numerous types of simulation [13]. One of its available modules provides the functionality of generating polyhedral meshes, suitable to be used within the environment of OpenFOAM. Moving to commercial platforms, there are a few that embed OpenFOAM mesh generation, and not only, procedures into their own functionality. However, probably the first and

most notable, so far, commercial implementation, is that of STAR-CCM+ [29], developed by CD-adapco, an early adopter of polyhedral meshes as a standard practice within their software.

Last but not least, through recent publications, automatic polyhedral mesh generation has received more attention [19, 10]. Garimella et al. are currently focusing their efforts towards a detailed description of polyhedral mesh generation methods [10]. Although their code has not, yet, been released, their contribution through publications has clarified the concepts of generating and optimizing polyhedral meshes, while ongoing research is being conducted for more advanced topics. Given the attention that polyhedral meshes have drawn during the past few years, more concepts and robust implementations are expected in the near future.

1.4 Background Theory

CFD is based on solving conservation equations for variables relevant to a fluid flow. These take into consideration sources and sinks, as well as the transport of material throughout the domain. Common variables of interest include mass, velocity, pressure, momentum, turbulent kinetic energy, turbulent energy dissipation rate etc.

The integral form of the generic conservation equation of a scalar variable ϕ takes the form of (Eq. 1.1) [6]:

$$\frac{\partial}{\partial t}\int_{\Omega}\rho\phi\, d\Omega + \int_{S}\rho\phi\boldsymbol{v}\cdot\boldsymbol{n}\, dS = \int_{S}\Gamma grad\phi\cdot\boldsymbol{n}\, dS + \int_{\Omega} q_{\phi}\, d\Omega \tag{1.1}$$

where t stands for time, ρ for the fluid density, $\boldsymbol{v}$ for the flow velocity, $\boldsymbol{n}$ for the unit normal vector of the surface S enclosing a Control Volume (CV) and Ω for the volume occupied by the CV. Γ is the diffusivity of quantity ϕ and q_{ϕ} represents the sources or sinks of ϕ.

Setting $\phi = 1$ and assuming no internal sources or sinks, the mass conservation equation occurs, in its integral form, which establishes the continuity of the

Control Volume (Eq. 1.2):

$$\frac{\partial}{\partial t}\int_{\Omega}\rho\, d\Omega + \int_{S}\rho\boldsymbol{v}\cdot\boldsymbol{n}\, dS = 0 \tag{1.2}$$

In a similar manner, for a fixed volume in space, the momentum conservation equation is formed by setting $\phi = \boldsymbol{v}$ (Eq. 1.3):

$$\frac{\partial}{\partial t}\int_{\Omega}\rho\boldsymbol{v}\, d\Omega + \int_{S}\rho\boldsymbol{v}\boldsymbol{v}\cdot\boldsymbol{n}\, dS = \sum\boldsymbol{f} \tag{1.3}$$

where $\sum\boldsymbol{f}$ represents the forces that act on the fluid contained in the volume. These can be surface forces, such as pressure, surface tension, etc., or body forces, such as gravity.

The application of these conservation equations is performed within the context of a method of discretization. There are various ways to formulate a solution scheme for CFD analysis. Historically, the oldest approach has been the Finite Difference Method. Despite being the simplest available, its restricted application to structured grids makes this method of little use for modern analysis of complex structures. Additionally, special care is required in order to apply the conservation principles on coarse grids, raising further restrains in commonly using a Finite Difference approach.

Another discretization scheme that can be used for CFD is the Finite Element Method. The advantage of FEM relies on the fact that arbitrary geometries can be easily handled and, with a robust mathematical background, many categories of CFD problems can be treated. It is ideal for diffusion dominated simulations, as well as viscous, free surface problems. However, it can be very slow for large problems, while it is not well suited for the analysis of turbulent flow.

The preferred approach of most CFD codes is that of the Finite Volume Method (FVM). In this method, the domain is subdivided into Control Volumes, to which the conservation equations are individually applied. Computations take place at the centroid of each Control Volume, where a value for the variable of interest is computed. The conservation equation, as applied in its integral form, becomes then (Eq. 1.4):

$$\int_S \rho\phi \boldsymbol{v} \cdot \boldsymbol{n}\, dS = \int_s \Gamma grad\phi \cdot \boldsymbol{n}\, dS + \int_\Omega q_\phi\, d\Omega \tag{1.4}$$

It should be mentioned, that the conservation equation is transformed from a volume to a boundary integral, whereas the sum of mass and impulse passing through the surface of the control volume, minus the contribution of any existing sources or sinks, must be zero [16].

The main advantage of FVM is that it is suitable for every type of grid, without limiting the cell shape, while the conservation equations are fulfilled even on coarse grids [2]. The simplicity of the method makes easy its algorithmic implementation, with well-developed iterative solvers guaranteeing its efficiency. However, one disadvantage of FVM is that it is not well-suited for higher order analysis. Finally, the fact that FVM is not restricted to using cells of specific shape is exactly the property that enables the use of polyhedral meshes.

Chapter 2

Mesh Topology and Representation

2.1 Introduction

The discretization of a continuum to a mesh model, which adheres to a respectful description of the geometry, is one of the most expensive steps in modern computational mechanics. A continuous effort is being made by researchers, in order minimize the storage and computing resources that are required during mesh generation. Furthermore, the structure of the mesh database that is used has a significant influence on performance, during the following steps of analysis and post-processing. Taking into consideration the way in which mesh entities need to be stored and, therefore, accessed, is not a trivial task and, in many cases, there is no straightforward answer as to what the optimum representation scheme is for a specific application. In most cases, demands in storage on the one hand, and efficiency on the other act in an competitive way, raising a question of minimizing storage requirements without sacrificing performance. In the following paragraphs, an attempt is made to present the basic concepts in mesh topology and clarify the needs of polyhedral mesh generation, regarding mesh data structures.

2.2 Definitions

2.2.1 Topological Entities

The topology of a mesh is an abstraction of the geometric model, that provides unambiguous, shape independent information about the relation between the entities that form the mesh structure. To this end, a mesh database is used in order to store various-level attributes of entities of different dimensions [7]. These typically include 0D entities, referred to, in literature, as *vertices* or *nodes*, 1D entities, referred to as *edges*, 2D entities, referred to as *faces* or *facets* and 3D entities, referred to as *solids*, *volumes*, *regions* or *cells*. In this study, the terms *vertex*, *edge*, *face* and *solid* are preferred.

2.2.2 Adjacent Entities

Each topological entity is bounded by a set of entities of lower dimension, forming a geometric object. Solids are bounded by faces, faces by edges and edges are bounded by vertices. Apart from this fundamental relation between entities, it is often useful to acquire a more advanced description of the relative connectivity that exists between the entities of a mesh structure. Even though in *Graph Theory* a distinction is made between different types of entities' relations, the term *adjacent entity* is uniformly used, in the context of mesh databases, to describe not only bounding entities but also directly connected neighboring entities of the same or higher dimension.

However, while for neighboring entities of lower dimension the adjacency relation unambiguous, connectivity information referring to entities of the same or higher dimensions may not always be unique. As an example, in a hexahedral mesh, a solid in the interior of a domain has 6 adjacent faces, 12 adjacent edges and 8 adjacent vertices. However, the adjacent solids of a hexahedron can be considered to be 6, those sharing common faces with, or 26, those sharing common edges with. It is, thus, important to define what is regarded as an adjacent entity within a certain context of use. Herein, connectivity of entities of the same or higher dimension, whenever needed, is described in a periphrastic way, in order

to avoid ambiguously interpreted relations.

2.2.3 Entities Classification

Mesh classification against the geometric domain is defined by the unique association of a mesh entity of dimension d_i, to a geometric model entity of dimension d_j, where $d_i \leq d_j$. Information about a mesh entity's classification allows for consideration of the original geometric model rather than the topological attributes of the mesh. This way, a direct link to the geometric shape information of the domain is achieved. A mesh entity is classified on a model entity, if it forms part or all of the discretization of the model entity [10].

Being able to acquire information about the classification of an entity, enables mesh generation algorithms to determine which mesh entities form the geometric model's boundaries, which lie entirely in the interior or even which are part of internal boundaries. This distinction of mesh entities yields useful information about their individual significance in the mesh's respectful representation of the geometric model and is essential in order to preserve the model's boundaries or other features, such as sharp edges or corners.

The classification of an entity is determined using its topological relation with adjacent entities of the same or other dimensionality. For three dimensional meshes, the origin for acquiring classification information about all entities is the classification of the faces of the mesh structure, which is then inherited by adjacent entities of lower or higher dimension. This concept is further described in (Sec. 2.4.3).

2.2.4 Notation

In the following, vertices, edges, faces and solids of a mesh are referred to as V, E, F, and S, respectively. A set of entities is enclosed within curly brackets "{ }" and adjacency relationships are represented by parenthesis "( )". As an example, a face of a solid can be referred to as F(S), while {F(S)} denotes the set of faces forming a solid. Finally, an arrow next to an adjacency relationship

Table 2.1: Notation of Adjacency Operators

Entity Type	*Solid*	*Face*	*Edge*	*Vertex*
Solids of	-	{S(F)} ↑	{S(E)} ↑	{S(V)} ↑
Faces of	{F(S)} ↓	-	{F(E)} ↑	{F(V)} ↑
Edges of	{E(S)} ↓	{E(F)} ↓	-	{E(V)} ↑
Vertices of	{V(S)} ↓	{V(F)} ↓	{V(E)} ↓	-

represent whether an upper or lower level entity is being accessed (Tab. 2.1) [7].

2.3 Mesh Representation Schemes

2.3.1 Explicit and Implicit Representation

Data structures that are commonly used to describe meshes can be divided into two major categories: *full* and *reduced representation schemes*. What differentiates the two is whether there exists an *explicit* way to access every level of mesh entities, or entities of one or more levels are omitted. Furthermore, for both categories, various ways may exist to describe the adjacency relationships between entities of the same or different dimension, providing a flexible way to access entities according to an application's demands. An explicit description of mesh entities of a certain dimension exists in the data structure, when there is at least one way to directly refer to the mesh entities. These faces can then be referred to by an index or identity number and iterators may be used to access the available information.

As an example, a data structure that contains information about the faces that exist in a 3D mesh is said to provide explicit access to the mesh's faces. This information may include the mesh's edges that form the boundaries of each face, provided that edges are also explicitly stored. Another possibility could be storing information about the mesh's vertices that form each face. There is, naturally, no restriction in explicitly storing both adjacency descriptions, however this would mean increased demand in memory, when access to face's vertices could have been achieved through the face's edges, being aware of their starting and ending vertex. On the other hand, when a certain entity level is omitted,

implicit access to the entities of that dimensionality may be possible. However, in this case, one would only be able to refer to them as adjacent entities of explicitly stored entities of a higher or lower level. If, in the previous example, information about mesh's edges is not stored in any way, there may be an implicit access to face's edges, given the face's vertices.

It is to be noted that, for every mesh entity of non-zero dimension, there should always exist an adjacency relationship, or a combination of them, that is able to explicitly or implicitly describe the entity's connectivity with mesh vertices. Although no theoretical restriction applies to describing a plain topological relationship, this demand emerges from the fact that, in structural modeling practice, a mesh is not a mere topological entity but a way to represent a corresponding geometric model. As, in common meshes, the only entities that contain geometric information are vertices, through their coordinates, it is always required that higher level entities are able to access vertices' information, otherwise the mesh entity would be geometrically undefined.

2.3.2 Full Mesh Data Structures

Data structures that explicitly store topological entities of all dimensions, namely vertices, edges, faces and, for 3D meshes, solids, are referred to as *full mesh representations*. Even though not all connections are always explicitly described, it is possible to implicitly retrieve adjacency information by combining the existing connectivity descriptions.

Full data structures require relatively high amount of storage space, compared to reduced data structures [7]. However, with modern systems specifications, describing geometric models in a satisfactory level of detail is usually not an issue, depending on the analysis type. On the other hand, computational effort, regarding mesh entities' connectivity, is significantly reduced, giving full mesh representations a noticeable advantage in performance [7, 8].

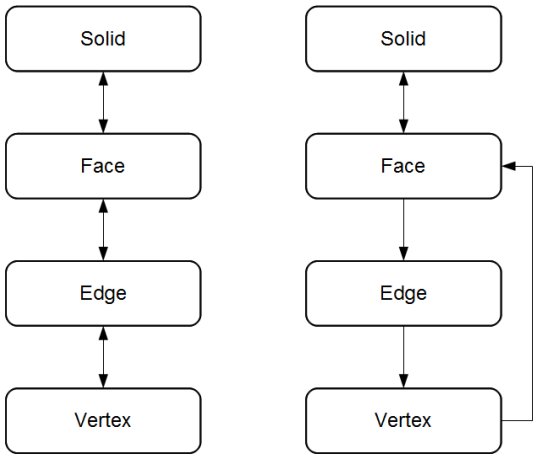

(a) F1 **(b)** F2

Figure 2.1: Common cases of full mesh representation schemes: explicit adjacency information is included for entities of all dimensions

2.3.3 Reduced Mesh Data Structures

Depending on the mesh information that an application requires, there are cases that not every level of entities needs to be accessed. Mesh data structures that omit one or more level of entities are referred to as *reduced mesh representations*. These entities may not be required at all, or their access may be seldom, so that they can be created on the fly whenever needed.

Reduced mesh representations have the advantage of significantly lower storage requirements, as compared to full representations [7]. However, the demand for implicit access to entities created on the fly increases the computational cost in a way that does not always counter-balance, in terms of overall performance, the low memory need [7, 8].

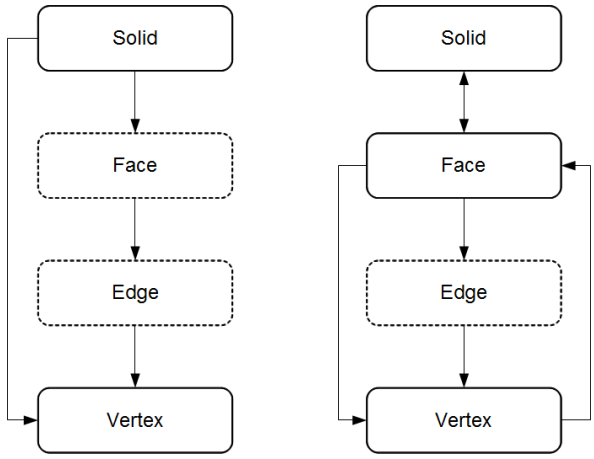

(a) R1 **(b)** R2

Figure 2.2: Common cases of reduced mesh representation schemes: adjacency information for implicitly represented entities is noted in dashed objects

2.4 Representation of Polyhedral Meshes

2.4.1 Data Structures

An important characteristic that a mesh data structure should have, is being able to effectively provide the necessary information required by the procedures that create and / or use that data. These needs can be different for various applications and are dictated by the information requests, made within the context of use.

One major problem with the commonly used element-vertex mesh data structures, is the lack of information relating the mesh entities to regions of the corresponding geometric model that are of special interest . More specifically, they provide insufficient information regarding the classification of primal mesh entities, which is of a decisive role during dual mesh generation. Furthermore, such representations are only functional with the aid of template-elements, that describe the relative position of a vertex within the element (Fig.2.3). It is apparent that for cells of arbitrary shape this cannot apply.

During polyhedral mesh generation, explicit access to mesh entities of all dimen-

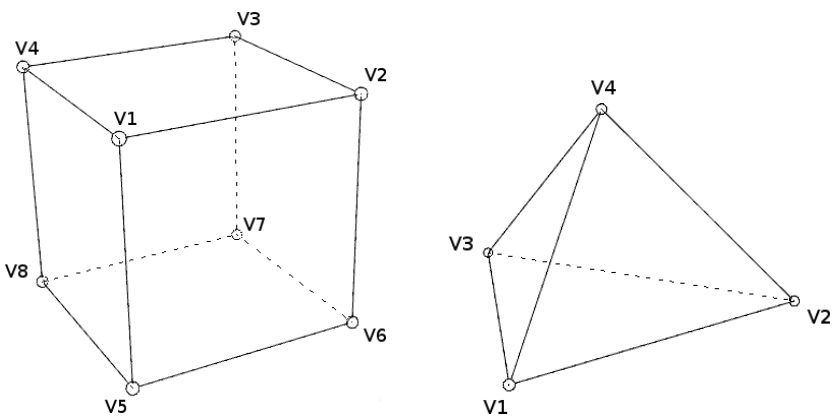

(a) Hexahedral element template

(b) Tetrahedral element template

Figure 2.3: Element adjacency templates

sions is required, as is described in detail in chapter (Ch. 3). Therefore, a full mesh data structure is needed, which allows for complete and fast access to mesh entities' adjacency relationship. The only restriction that applies, when selecting among different full representation options, is that solids must be explicitly aware of their faces, or, in other words, the relationship {F(S)} that corresponds to the polygons that form a polyhedron cannot be described in an implicit way. The reason behind this restriction is that polyhedral shapes are, in general, arbitrary, with solids of the same mesh having different numbers of faces. What is more, the polygonal faces themselves have varying numbers of edges and vertices. Thus, it is not possible to establish {E(S)} or {V(S)} relationships in a predefined way throughout the mesh, as opposed to meshes of elements with pre-defined shape.

In a pure hexahedral or tetrahedral mesh, for example, an explicit {V(S)} adjacency description would be possible, by storing the vertices of each element in locally consistent positions (Fig. 2.3a, 2.3b). By forming such a pre-defined {V(S)} template, all other adjacency relations is possible to be derived on the fly.

As far as polygonal faces are concerned, even though {E(F)} and {V(F)} adjacency relationships cannot be locally predefined as well, the fact that faces are required to have a counter-clockwise orientation guarantees that it is always possible to access a face's edges or vertices in the correct order, knowing which entity is at which relative position.

Finally, the most often requested adjacency relationships refer to entities of one or two levels apart and, thus, it makes sense to explicitly describe them. Two well qualified candidates are, therefore, the mesh representations depicted in (Fig. 2.1a, 2.1b), from which the former has been chosen, within the scope of the present work, due to it's simpler design and the more intuitive hierarchical order.

Therefore, a mesh database, herein, explicitly contains entries for existing vertices and their coordinates, edges defined by their bounding vertices, faces defined by their bounding edges and solids defined by their bounding faces. Additionally, a face is aware of the solids it is adjacent to, an edge is aware of the faces it is adjacent to and a vertex is aware of the edges it is adjacent to. Every other connectivity relation is implicitly retrieved by making use of the above, explicitly stored information.

2.4.2 Adjacent Entities Orientation

It is common for mesh entities of certain dimensions to be defined in a way that describes their orientation in space. For example, when faces stored in a mesh database, it is done so in an ordered manner, meaning that the edges and vertices that describe them are accessed in a counter-clockwise sequence that denotes a positive definition of the faces' orientation. It is also of common practice that each solid within a mesh is bounded by 2D entities that are always facing outwards, or that they are positively oriented with respect to the solid. These are conventions that allows for a unified consideration of the relative definition between adjacent entities.

Therefore, when a face is accessed as an adjacent entity of a solid, it is necessary to know if the counter-clockwise definition of the face coincides with the definition that denotes a positive orientation with respect to the solid it bounds. If this is the case, then the adjacent face is marked as positively oriented, usually setting a +1 flag in the solid-face adjacency information. Otherwise, it is negatively defined and a -1 flag is set, which will be considered to access, from the solid's perspective, the adjacent face's edges or vertices in the opposite sequence that the face is defined within the mesh structure database.

Similarly, edges are usually stored, knowing their starting and ending vertices. For a face to properly access the vertices of one of its adjacent edges, it needs to be aware of whether the orientation of the edge, as stored in the database, is respectful to the counter-clockwise that the face should have, or if it is oriented the opposite way. A +1 / -1 flag is then stored for respective face-edge adjacency information.

Finally, the same applies for the vertices of the mesh, where a +1 flag is noted for an adjacent edge of which the vertex is its starting point, and a -1 for an adjacent edge that uses this vertex as an ending point. However, in this case, this relation of orientations can be dynamically retrieved, by the information stored in the edge, and no flag needs to be stored on the vertex side.

2.4.3 Boundary Detection

Although solids cannot be classified on a boundary surface, as they are always in the interior of the model, those solids whose at least one adjacent face is classified on the boundary can be detected by iterating through their faces. These solids form the boundary layer of the geometric model, which is of special interest in CFD simulations, thus it is often useful to be able to detect them.

A face is said to be classified on the boundary of the geometric model, when it is adjacent to only one solid, which means that the "free" side of the face forms an external boundary. In the opposite case, where a face is adjacent to two solids, it is classified in the interior of the geometric model. Additionally, it is common in mesh generation to assign specific attributes to faces classified on the same model boundary surface, referring to them under the same boundary identifier, usually group number. This way, it is topologically possible to access mesh faces that form a common model boundary and distinguish them from faces on other boundaries.

Mesh edges inherit their classification by their adjacent faces. Specifically, when an edge has at least one adjacent face that is classified on a model's boundary surface, the edge is also classified on the same boundary. To be more precise, in a conforming non-manifold three-dimensional mesh, an edge will have either zero or at least two adjacent *boundary* faces, however detecting one of them can

be considered enough to classify the edge on the boundary as well.

Furthermore, when an edge's adjacent boundary faces are classified on different boundary surfaces of the model, this denotes the edge's classification on a model's boundary edge, where two of its boundary surfaces intersect. It is, therefore, adequate to count the amount of different boundary identifiers that are assigned to the adjacent faces of an edge, in order to conclude whether this edge is internal (zero boundary identifiers), on a boundary surface (one identifier), on a boundary edge (two identifiers), or is a non-manifold edge (more than two identifiers).

Extending the aforementioned classification criteria for vertices, a mesh vertex is classified on a model's boundary surface, when at least one of its adjacent edges is also classified on a boundary surface. Additionally, when at least one of the adjacent edges of a vertex is classified on a model's boundary edge, then the vertex is also classified on the same boundary edge. Finally, when there exist at least two adjacent edges classified on two different model's boundary edges, the vertex is classified on a model's corner, formed at the intersection of the boundary edges.

In other words, the classification of a vertex with respect to the model can be determined by counting the amount of different boundary identifiers assigned to the adjacent faces of the vertex. Zero boundary identifiers denote an internal vertex, while vertices on a boundary surface have adjacent faces with a unique identifier. Nodes on model's boundary edges have adjacency relationships to faces of two boundary identifiers in total and vertices on a model's corner sum up with three adjacent boundary identifiers. Finally, when a vertex has adjacent faces classified to more than three different boundary surfaces, the vertex is non-manifold.

2.4.4 Significant Entities

In the previous chapter (Ch. 1), an overview of the principles behind polyhedral mesh generation was given, where the distinction was made between primal entities that contribute to the generation of dual vertices. All types of primal entities, depending on their classification, participate in forming dual entities, and affect the topological connectivity of the obtained mesh. However, those

primal entities that participate in the generation of dual vertices are of special interest, as they form the main contributors to the definition of the geometry of the dual mesh. This comes as a consequence of the fact that dual vertices will be the only dual entities that will contain geometric information: their coordinates.

This distinction is made by defining the criteria under which a primal mesh entity is considered to have important geometric properties that need to be preserved in the dual mesh. In this context, they are referred to as *significant* primal entities. These can be of any dimension and classification, however they are distinguished by certain combinations of characteristics that make them special. Usually, they are classified on the geometric model's boundaries or boundary intersections and they contribute a central point within their local domain, that becomes a dual vertex. However, it is up to the user to determine the exact criteria that will form the vertices of a dual mesh, allowing, this way, for flexibility over the mesh generation.

Primal solids are always regarded as significant and each contributes a dual vertex in a central point within its volume. Their union represents the domain of the geometric model and they are the generators of all dual vertices that will lie in the interior of the dual mesh, once the polyhedral mesh generation is complete.

Significant primal faces are those that are classified on the geometric model's boundary surfaces, and can be detected as described in (Sec. 2.4.3). Each significant face contributes a dual vertex lying on a central point within its area. The resulting vertices are classified on the model's boundaries as well, and are those that will define the boundary surfaces' geometry for the polyhedral mesh.

The primal edges, the geometry of which needs to be preserved in the dual mesh, are those that are classified on the boundary edges of the geometric model or, in other words, on the boundary surfaces' intersections. They constitute a subset of the edges classified on the boundary, that are connected to two or more significant faces that belong to different boundary surfaces. Except for the fundamental topological criteria, geometric criteria may apply as well. A common practice is to mark a primal edge as significant, when two of its adjacent significant or boundary faces form an angle that is smaller than a predefined value, regardless of the surface they are classified on. Depending on the implementation and the analysis prerequisites, more geometric criteria may apply.

Finally, significant primal vertices are those that are classified on the geometric model's corners or, in other words, lie on significant edges' intersections, when these edges are connected, in total, to three or more different boundary surfaces. This is something that can be detected as in the previous case, of significant edges. Significant vertices contribute an exact copy of themselves to the polyhedral mesh, and their role is to preserve the model's corner. In a similar way as with significant edges, additional geometric criteria may apply, as well, for the detection of significant vertices. A common case considers primal vertices that are connected to significant or boundary edges that form an angle that is smaller than a predefined value.

Chapter 3

Polyhedral Mesh Generation

3.1 Introduction

One thing to consider, when it comes to mesh generation, is the distance that often exists between the mathematical description of a method and its algorithmic implementation for a specific field of application. This has also been the case with polyhedral mesh generation, which, despite the existence of thorough research, regarding its fundamental principles, it has yet to become a common choice of analysts in CFD simulation. One important factor for this is the lack of a broad selection of polyhedral mesh generators that analysts could choose from, as challenges regarding the implementation of such tools, suitable for CFD analysis, still exist. Recently, an attempt to publicly address current issues in generating polyhedral meshes has been made, suggesting a robust methodology in mesh generation [10]. Having this progress in mind, an independent study in polyhedral meshing has been made in the present work, which has resulted to the implementation of a polyhedral mesh generator. The basic steps that have been followed, as well as the challenges that have been encountered, are described in the following paragraphs.

3.2 Methodology

As previously described, the topology of a polyhedral mesh depends on that of a primal mesh, forming its dual counterpart, according to a set of predefined rules that form a duality transform mapping. Each dual entity corresponds to a primal counterpart entity, depending on the properties of the latter. Consequently, by applying the same set of rules, a primal mesh will always result to the same dual mesh.

Given a triangular mesh in 2D, such as that of (Fig. 3.1), a polygonal mesh is formed, following the principle that a dual cell will be formed around every primal vertex . In the interior of the domain, this one-to-one correspondence between primal and dual entities extends to other types as well, with one dual edge per primal edge and a dual vertex for every primal face. However, generation of polygonal faces on the boundary demands for additional dual edges and vertices, at specific locations of the boundary that denote the classification of primal entities as significant. An algorithmic description of the general procedure, for the 2D case, is, then, as follows:

1. All primal faces are considered significant. A dual vertex is created at a central point of every primal face.
2. Primal edges classified on the boundary are considered significant. A dual vertex is created at the midpoint of significant primal edges.
3. Primal vertices classified on boundary intersections are considered significant. A dual vertex is created for every significant primal one, coinciding with it.
4. A dual edge is created for every pair of adjacent primal faces, by connecting the dual vertices created at their central points, crossing their common primal edge.
5. A dual edge is created for every significant primal edge, by connecting the dual vertex created at its midpoint with the dual vertex created at the central point of its single adjacent primal face.

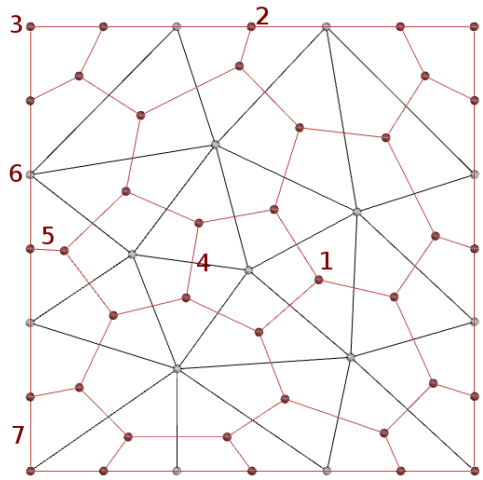

Figure 3.1: A primal triangular mesh and its general polygonal dual

6. A dual edge is created for every pair of adjacent significant primal edges classified on the same boundary, by connecting the dual vertices created at their midpoints.

7. A dual edge is created for every significant primal edge classified on a boundary intersection, forming a corner of the geometric model, by connecting the dual vertex created at its midpoint with the dual vertex on the boundary intersection.

8. A dual face is created for every primal vertex, by collecting the dual edges that connect the dual vertices, which correspond to the adjacent faces of the primal vertex (generated in step 4).

9. If the generator primal vertex is classified on a boundary or a boundary intersection, the dual edges classified on the same boundary are additionally considered, in forming the dual face (generated in steps 5 – 7).

A slightly modified approach of the generic polygonal mesh generation, as previously described, is used to obtain a variation known as median meshes. This method differentiates itself by considering as significant every existing primal edge, thus creating dual vertices at the midpoints of primal edges lying in the interior as well. These dual vertices become, consequently, vertices of the dual faces formed around primal vertices in the interior, however the resulting polygons are characterized by highly concave shapes (Fig. 3.2).

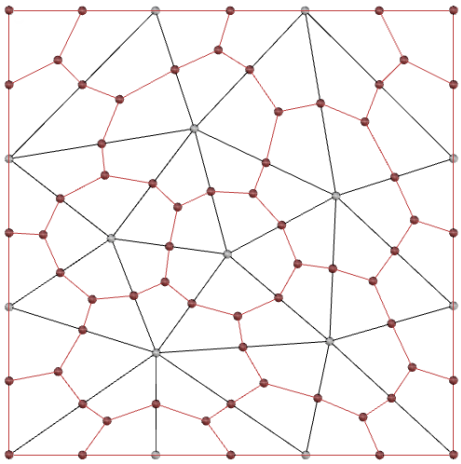

Figure 3.2: A primal triangular mesh and its median polygonal dual

Concave polygons are in general non-desirable in computational methods, due to their poor numerical properties. Additionally, they are also known for posing further difficulties in geometric computations, making the mesh generation itself problematic, whenever using plain topological relations is not adequate. It is, subsequently, clear that median meshes are not an optimal choice for numerical simulations. However, the concept behind median mesh generation provides a useful basis for meshing curved boundary surfaces of three-dimensional models, where the exact geometry of the primal mesh needs to be preserved. This topic, as well as avoiding further computational geometry difficulties due to concave polygons, are discussed in (Sec. 3.5.1).

3.3 Primal Mesh Generation

A primal mesh can be any valid mesh which will serve as input for the polyhedral mesh generation algorithm. In the present work, the case of conforming, possibly mixed, manifold meshes has been considered, whether structured or unstructured, although other studies have shown the applicability of the same methodology, with slight modifications, to non-manifold meshes as well [10].

As the primal purpose for generating polyhedral meshes lies on the need for high quality meshing of arbitrary 3D domains in CFD simulations, focus has been

placed on tetrahedral primal meshes, which are flexible in representing complex geometries. Given the fact that the quality of the input mesh influences directly the output, a high quality tetrahedral mesh generator is a prerequisite towards polyhedral meshing. Furthermore, in order to obtain characteristics as close as possible to a Voronoi tessellation, even though it is not possible to achieve an exact meshing of such kind, a mesh generator capable of deriving a Delaunay tetrahedralization is preferred.

Generating a qualified primal mesh, suitable to form a basis for deriving a polyhedral dual mesh, does not require any method that the modern analyst is not familiar with. Already available mesh generation tools are capable of delivering high quality meshes. To this end, in the present work, NETGEN mesh generator has been used for generating tetrahedral primal meshes [18] [27].

3.4 Dual Mesh Generation

Dual meshes are generated in a hierarchical order, starting from 0D up to 3D entities, given criteria that emerge from primal entities classification. The fundamental concept, as an extension to the two-dimensional case, is to create dual volumes around every vertex of the primal mesh, establishing this way a one-to-one correspondence between them. The way to obtain dual entities is described in details in the following paragraphs.

3.4.1 Dual Vertices

Every cell of the primal mesh, whether classified on the boundary or in the interior, is considered a significant entity, resulting to a corresponding dual vertex, created at a central point of the primal volume. Common choices where dual vertices can be positioned are primal volumes' centroids or, in the case of tetrahedra, their circumcenters are an alternative option. The selection of central points is crucial for the quality of the resulting polyhedral volumes and is discussed in more detail in (Sec. 4.3.1). Dual vertices in the interior are generated by parsing through every cell of the primal mesh and computing its central point.

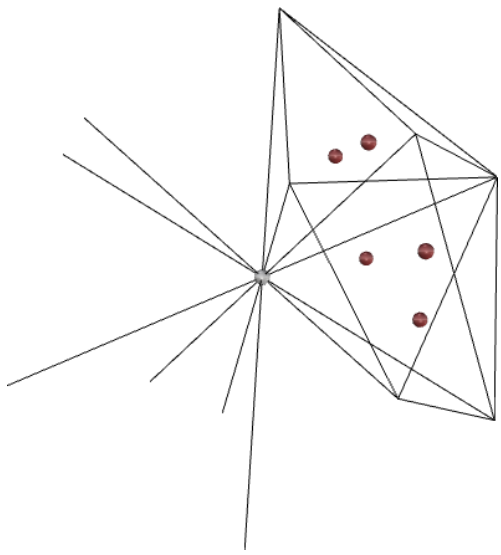

Figure 3.3: Generation of internal dual vertices

Every face on the boundary of the primal mesh will be considered during dual mesh generation by contributing its central point. As is also the case with central points of volumes, the selection of central points of boundary faces has a decisive effect on the shapes of the dual polygons that will be formed on the boundary. Common central points are primal faces' centroids or, in the case of triangles, their circumcenters can be also used. Dual vertices of this classification are generated by parsing through every primal face of the source mesh and considering those classified on the model's boundary. This is achieved by evaluating if a face is connected to one, and only one, primal volume.

Primal edges on a boundary edge of the model contribute their midpoints in order to form dual vertices. These dual vertices are generated by parsing through every primal edge and considering those classified on a model's boundary edge. This is achieved by evaluating if two of their adjacent primal faces are classified on two different boundaries of the model.

Finally, dual vertices are created coinciding with primal vertices at positions where the model's boundary edges intersect, forming "corners" of the model. These vertices are generated by parsing through every primal vertex and considering those classified on a model's boundary edge intersection. This is achieved by evaluating if at least two of their adjacent primal edges are classified on different boundary edges of the model, which is, in turn, evaluated by verifying that

the edges' adjacent faces, in total, are classified on at least 3 boundary faces of the model.

3.4.2 Dual Edges

Dual edges in the interior are generated by connecting the central points of all adjacent primal volumes. This is achieved by parsing through all primal faces and, for those that are in the interior of the model, being connected to two primal volumes, a dual edge is generated by connecting the central points of their adjacent volumes.

Additionally, dual edges in the interior are generated, corresponding to primal faces classified on the boundary, having only one adjacent volume. For these primal faces, a dual edge is created by connecting their central point with the central point of the adjacent volume.

For every primal edge that is classified on the boundary, a dual edge is created on the boundary, as well, when the primal edge is connected to two faces classified on the same boundary. In this case, a dual edge will be generated, connecting the central points of these faces and crossing the generator primal edge.

In case that a primal edge is classified on a model's boundary edge, dual edges will be generated, connecting the midpoint of the generator primal edge with the central points of primal faces classified on different boundaries.

For primal vertices classified on a model's boundary edge, a dual edge on the same boundary will be generated, by connecting the midpoints of two primal edges, when these are classified on the same boundary edge of the model.

Finally, corresponding to primal vertices on a geometric model's corner, dual edges will be generated, connecting the coinciding dual vertex on the corner with the midpoint of every primal edge classified on a model's boundary edge.

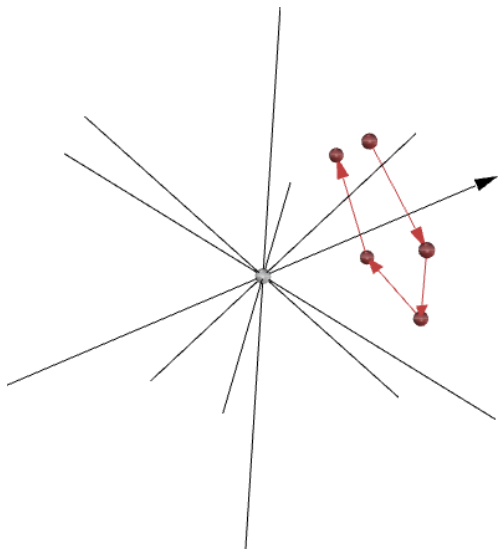

Figure 3.4: Generation of internal dual edges

3.4.3 Dual Faces

Dual faces in the interior are generated by collecting the dual edges that have been created, by connecting the central points of the primal volumes surrounding primal edges. This is achieved by parsing through primal edges and, for every connected primal face, the corresponding dual edge is collected. When all dual edges surrounding a primal edge have been retrieved, they have to be sorted according to their vertices, following a counter-clockwise orientation.

For primal vertices classified on a model's boundary surface, a dual face is generated, by collecting all the dual edges surrounding a vertex, that are also classified on the same boundary. These dual edges correspond to primal edges connected to the primal vertex, that are also classified on the same boundary.

Furthermore, for every primal vertex classified on a model's boundary edge, a dual face is generated for every set of connected primal edges that are classified on the same boundary surface, considering also those classified on the boundary edge. The dual edges corresponding to each set of primal edges are collected and sorted around the primal vertex, using as a reference vector the mean of the normals of the faces classified on the corresponding boundary surface.

Finally, primal vertices classified on the geometric model's corners, where the

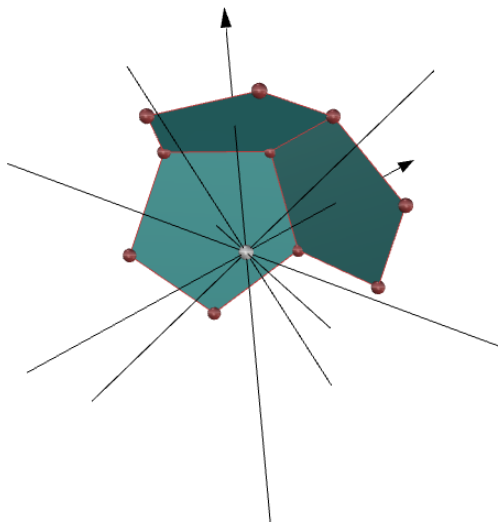

Figure 3.5: Generation of internal dual faces

edges of the model intersect, result to the formation of one dual face for every intersecting boundary surface. Each dual face is formed by collecting the dual edges that connect the centers of primal faces classified on the same boundary, as well as the dual edges connecting the same centers with the midpoints of significant primal edges. Additionally, the dual edges connecting these midpoints to the dual vertex on the corner are considered, in order to form a closed dual face.

3.4.4 Dual Solids

After dual entities of all lower dimensions have been created, polyhedral volumes are formed around every vertex of the primal mesh. This is achieved by iterating through the primal edges connected to each registered primal vertex. The dual faces, which have previously been generated and correspond to primal edges, are collected, forming the boundaries of the dual volumes. In the case of primal vertices on a model's "corner", the dual faces corresponding to the primal vertices are considered as well.

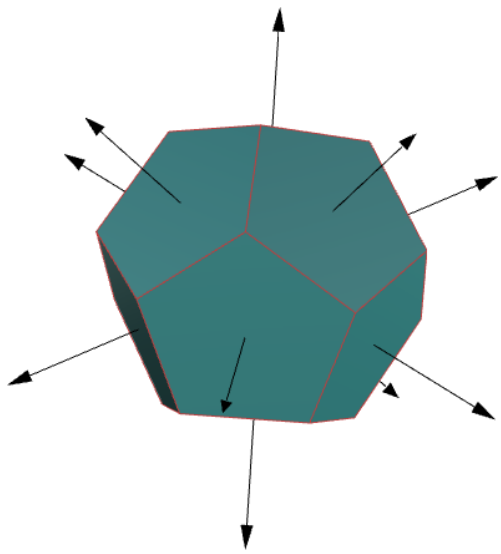

Figure 3.6: Generation of internal dual cells

3.5 Special Considerations

The resulting polyhedral mesh of an indirect mesh generation method depends vastly on the properties of the primal mesh. This allows for little flexibility regarding the parameters that control the overall procedure. Nevertheless, given the fact that modern direct mesh generator codes are able to provide high quality tetrahedral meshes, the geometric properties of resulting dual meshes are, in general, acceptable.

Following the guidelines described in the previous paragraphs, a conforming polyhedral mesh is obtained, which respects the model's boundaries as represented by the primal mesh. It is, however, essential that the geometric properties of the resulting mesh entities are such that no numerical instabilities or errors are introduced, when a CFD analysis is conducted. Common problematic issues are the generation of concave or non-planar faces and the corresponding non-convex polyhedra that may be created.

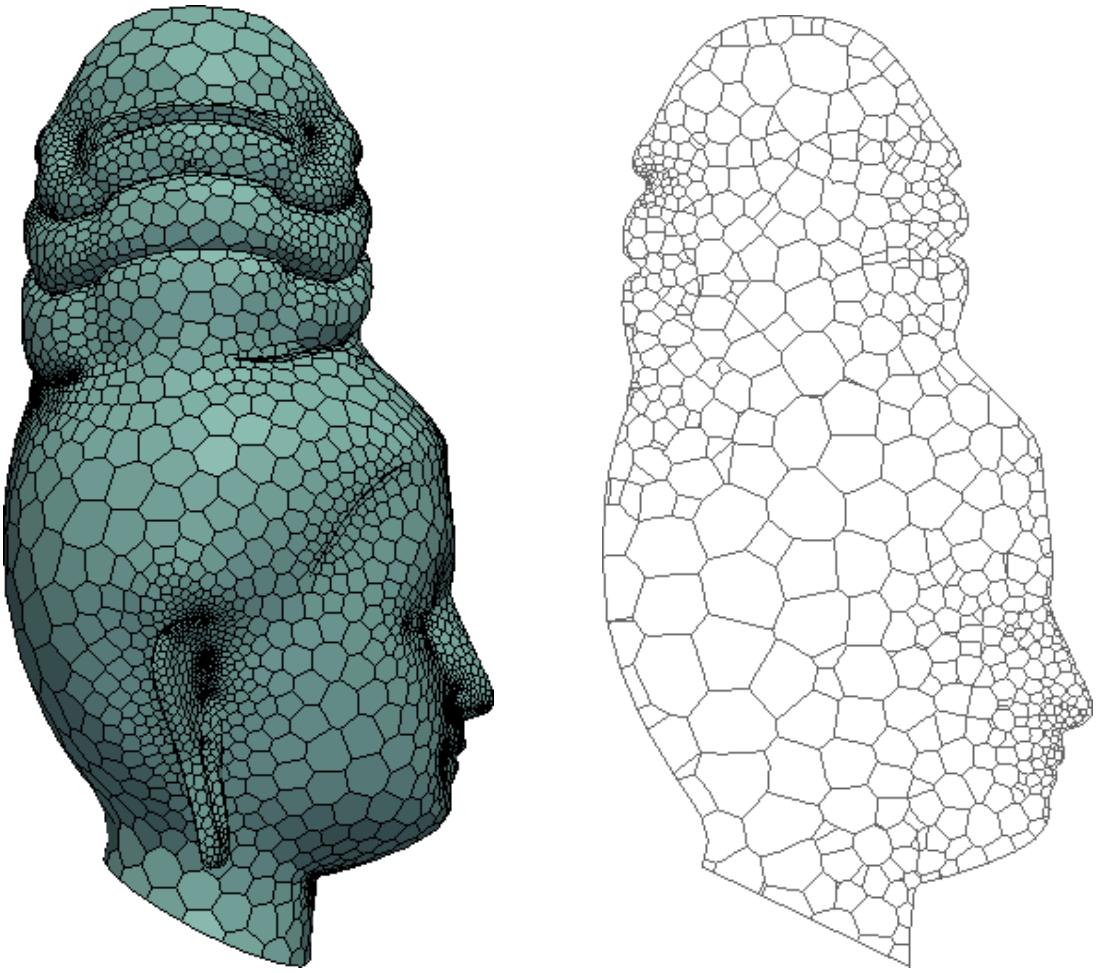

(a) Dual mesh **(b)** Slice of dual mesh

Figure 3.7: Polyhedral mesh of a complex geometry in 3D

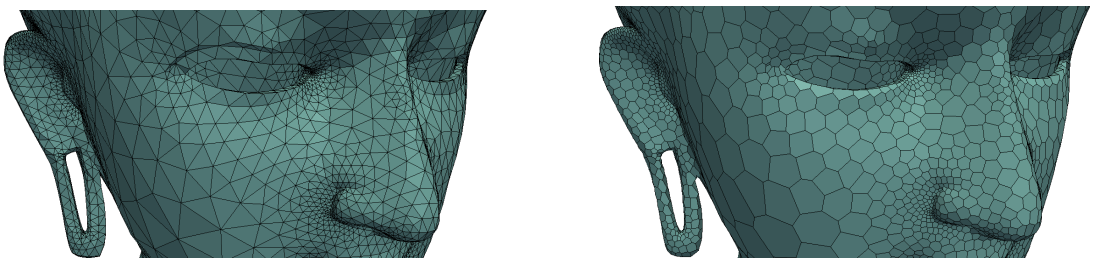

(a) Tetrahedral primal mesh **(b)** Polyhedral dual mesh

Figure 3.8: Meshing details of a complex geometry in 3D

3.5.1 Preservation of Boundaries

One important aspect of mesh generation methods is how respectful are the resulting meshes to the geometry of the domain that they represent. Especially for studies that involve interaction of fluid flows with solid objects, as is usually the case with CFD, the geometric properties of the solid object models on their boundaries are crucial for the quality and validity of the analysis in its whole. One can consider, for example, the significance of the precise representation of the flight control surfaces within the aerospace engineering discipline, or the boundaries of blood vessels in computational medicine. Deriving from an indirect mesh generation, a polyhedral mesh can only respect the domain's geometry up to the degree that its primal counterpart mesh does. Assuming a respectful primal mesh, with regard to the geometric model, it is desired that, in turn, the dual mesh is as respectful as possible to the primal mesh.

Considering a curved boundary surface, such as in figures (Fig. 3.9, 3.10), the fact that entities of 1st polynomial order are used in both counterpart meshes guarantees that the two representations of the boundary can not coincide. A smoothening of the primal mesh boundary is introduced, which, depending on its extent and the nature of the analysis, may or may not be of importance. Furthermore, due to the exact same effect, the volume of the total mesh is altered, increasing or decreasing, depending on the curvature sign of the surface. The degree up to which this inflation or deflation appears, depends not only on the curvature but also on the fineness of the meshes. In general, though, this approximation of the dual mesh, regarding the primal mesh boundary surfaces, follows in quality the approximation of the primal mesh, regarding the geometric model boundary surfaces, leading to acceptable dual representations in most cases. A way to be able to control such effects is, nonetheless, desired.

Of higher impact to the geometric properties of the mesh in CFD analysis is the respectful representation of the geometric model's boundary edges, which have a direct and significant influence on flows around them. The primal mesh edges that represent a model's boundary edge are, themselves, an approximation of the domain's geometry and, for the same reasons as with surfaces, their dual counterparts will, inevitably, introduce a longitudinal smoothening of the boundary along its path. This is usually also acceptable, as long as the boundary edge is

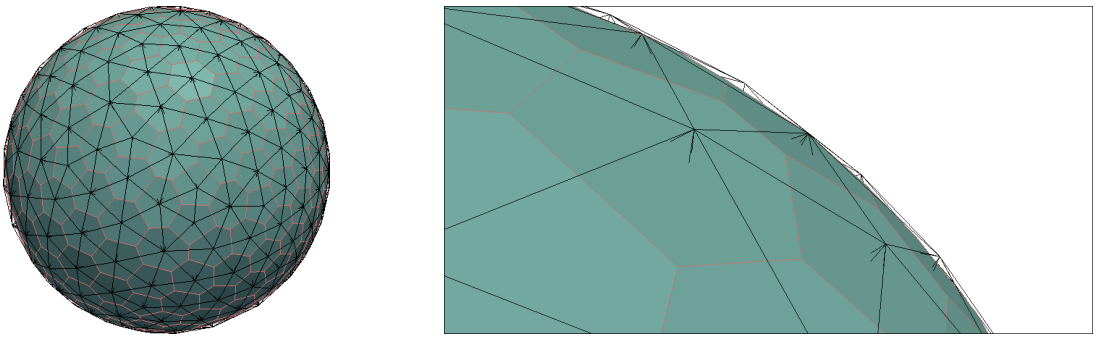

(a) Coarse mesh **(b)** Detailed view of coarse mesh

Figure 3.9: Volume deflation of $\approx 2.0\%$ due to a curved boundary surface

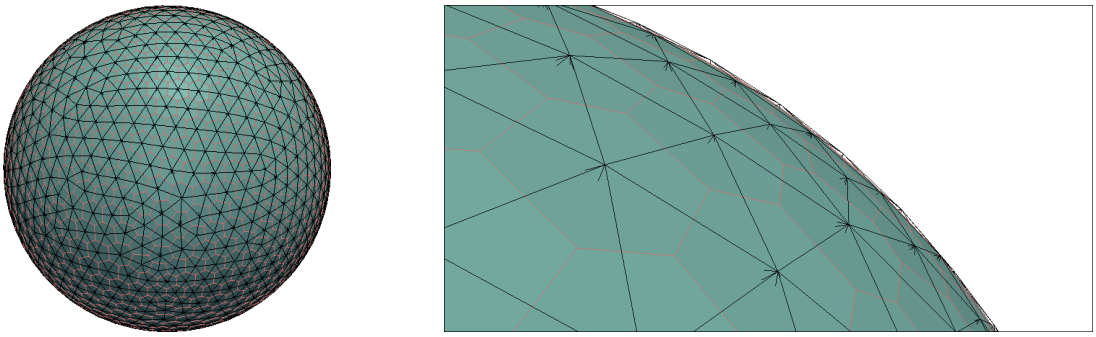

(a) Fine mesh **(b)** Detailed view of fine mesh

Figure 3.10: Volume deflation of $\approx 0.5\%$ due to a curved boundary surface

preserved and continues to be represented in the dual mesh. There is, hence, the requirement that it is not truncated by introducing a transverse smoothening across the intersecting boundary surfaces, following the same concepts as in the case of boundary surfaces.

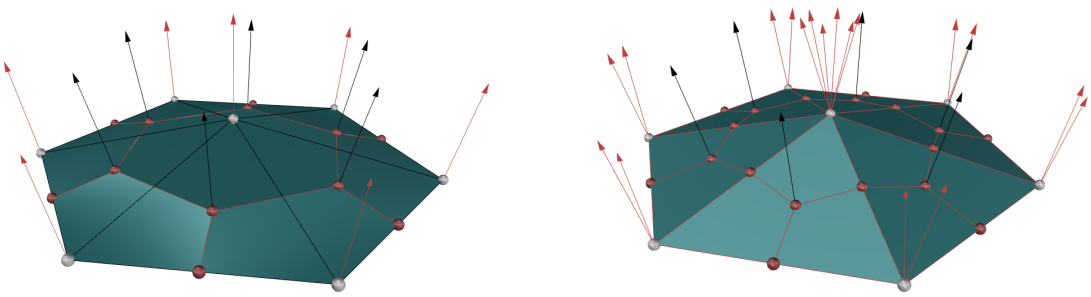

(a) Smoothening of boundary surfaces **(b)** Preservation of boundary surfaces

Figure 3.11: Preservation of the geometry of primal mesh surfaces

In (Ch. 3), explicit consideration is taken when referring to dual entities generated on the geometric model's boundary edges, in order to ensure the boundary's preservation in the dual mesh. This is achieved by detecting primal generator-entities that are adjacent to significant primal edges. By the term *significant*, as explained in (Sec. 2.4.4), is implied that these primal edges will not only contribute their midpoints as dual vertices but will also result to a corresponding dual entity classified on the same boundary.

The detection of significant edges is determined by the fact that they are adjacent to boundary faces that are classified more than one boundary surface. It is, consequently, required that, during pre-processing, all primal faces on the same boundary surface are assigned the same boundary identifier, which is different for every boundary surface. This a feature supported in most commonly used tetrahedral mesh generators. As an additional criterion, a primal edge may be marked as significant when its adjacent boundary faces form an angle greater than a specified amount.

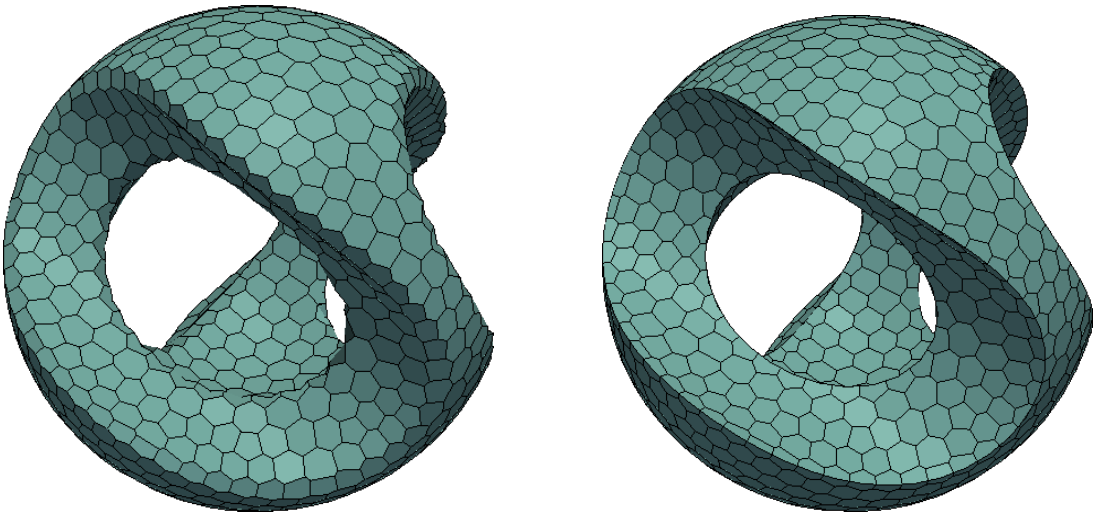

(a) Transverse smoothening of significant edges

(b) Preservation of significant edges

Figure 3.12: Preservation of the geometry of primal mesh edges

3.5.2 Internal Boundaries

Special care is required at areas where boundaries are present, within the 3D domain. In general, two different situations may result in the formation of internal boundaries, which require separate treatment.

One case includes voids completely enclosed by the 3D volume. Even though these voids form geometric boundaries that are in the interior of the domain, from a topological perspective they can be treated exactly the same way external boundaries are. Such areas, that denote a distinction between the continuum material and the absence of it, can be detected by assigning a boundary condition and orienting external faces in such a way, that their normals point away, with respect to the volume. In case of internal voids, it is sufficient that these normals, already at the primal mesh, point towards the void "center" and not the material (Fig. 3.13a – 3.13c).

However, there are cases where an internal surface is not used in order to distinguish between continuum or void areas, but rather to differentiate between areas with different materials. Furthermore, internal boundaries may also be used to explicitly state that a region within the domain should be preserved as in the primal mesh, as elements of special interest are classified on this boundary. As an example, this approach may be desired in order to preserve a region where two blocks of different primal element types, within a mixed mesh, meet. Currently, the present implementation is not designed to handle such cases, however it has been shown that with slight modifications, regarding the polyhedral mesh generation rules, it is possible to account for this consideration [10].

3.5.3 Boundary Layer

The poor numerical properties of tetrahedral meshes have dictated the generation of a thin layer of prismatic, pentahedral elements at the boundary. With this common practice, analysts have been able to partially overcome the inability of tetrahedra to capture the details of a flow at regions close to the boundary [23].

The appropriate generation of a corresponding boundary layer for polyhedral

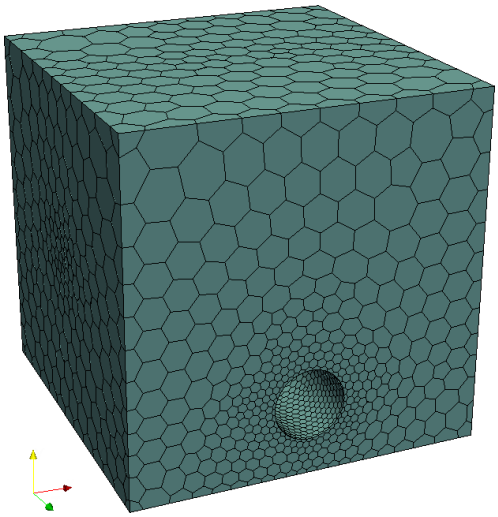

(a) External look of the mesh

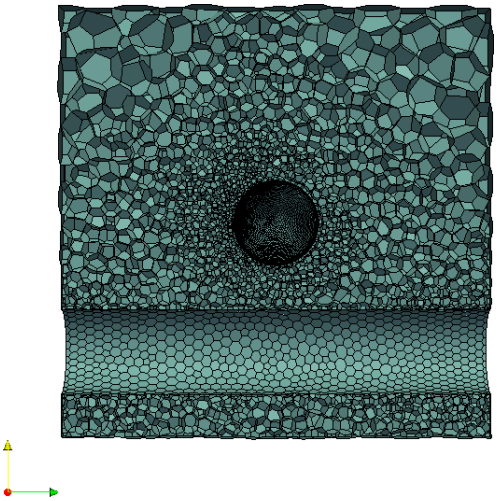

(b) Cut along main axis of cylindrical hole

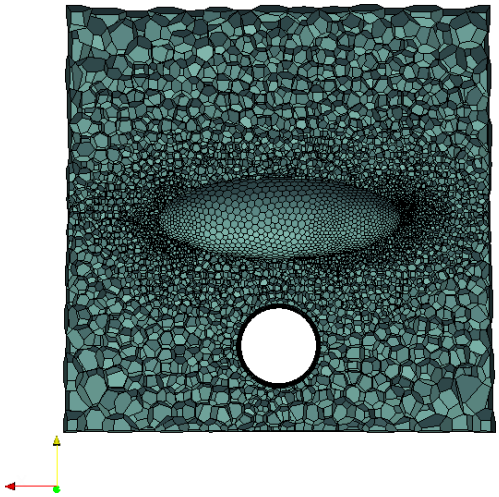

(c) Cut across main axis of cylindrical hole

Figure 3.13: Polyhedral mesh with cylindrical hole and internal elliptical void

meshes, or even the need for one, are to be examined in future studies. An interesting, however, by-product of the polyhedral mesh generation method, is the automatic formation of a prismatic boundary layer. This effect comes as a result of connecting the centers of primal cells, in order to form dual entities, which, at the boundary, forms dual cells of approximately half the thickness of their primal counterparts.

The phenomenon can be intensified by generating cascading dual meshes, having as a starting point an initial primal mesh. This is made possible, given the ob-

servation that the dual counterpart of a general bounded polyhedral mesh tends to resemble the primal, tetrahedral mesh, with the exception at the boundaries. This correspondence emerges in a similar way that the dual counterpart of a Voronoi tessellation is a Delaunay triangulation / tetrahedralization, and vice versa. Therefore, for each generation of meshes, the dual mesh that is obtained serves as the primal mesh for the next iteration.

It can, then, be observed that for each generation, the boundary layer gets approximately half the thickness of that of the input mesh. Since two iterations are needed in order to cascade from a polyhedral mesh to a tetrahedral dominant and back to a polyhedral one, the formed boundary layer will conclude to a thickness of a $\frac{1}{4}$ factor. It is, however, apparent that with such an approach it is difficult to control the properties and thickness of the formed boundary layer and the application of this method seems of limited use.

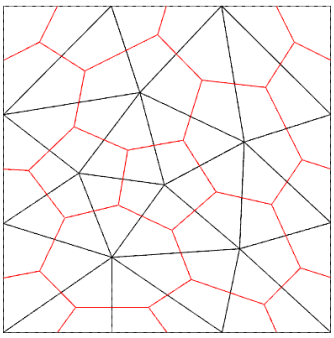

(a) Triangular primal mesh (black) and 1st generation polygonal dual mesh (red)

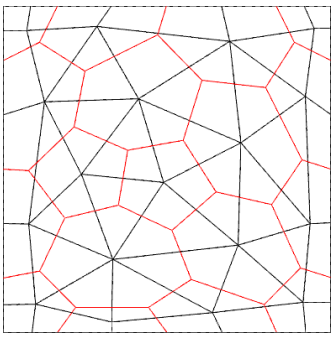

(b) 1st generation polygonal dual mesh (red) and 2nd generation triangular dominant dual mesh (black)

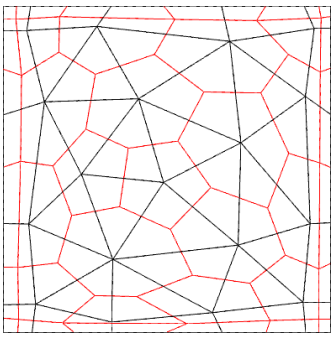

(c) 2nd generation dual mesh (black) and 3rd generation dual mesh (red)

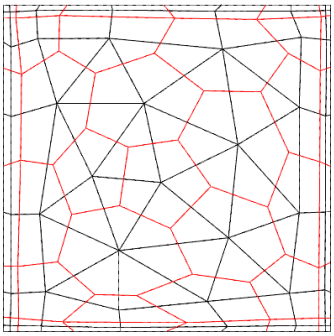

(d) 3rd generation dual mesh (red) and 4th generation dual mesh (black)

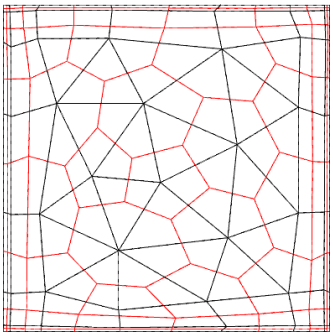

(e) 4th generation dual mesh (black) and 5th generation dual mesh (red)

Figure 3.14: Formation of boundary layer with cascading mesh generation in 2D

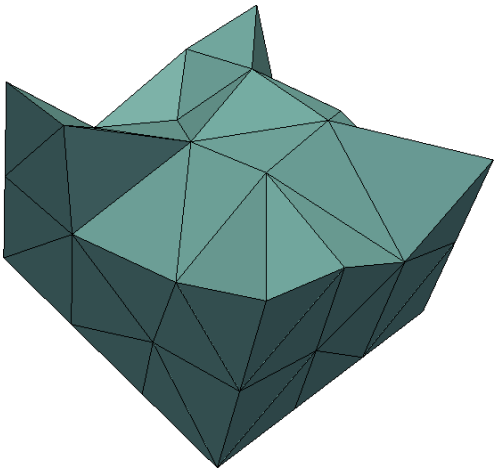

(a) Tetrahedral primal mesh

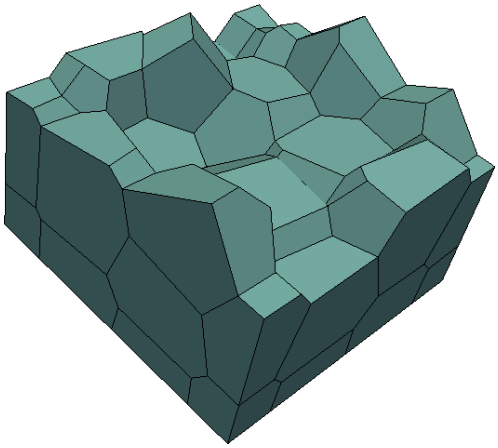

(b) 1st generation polyhedral dual mesh

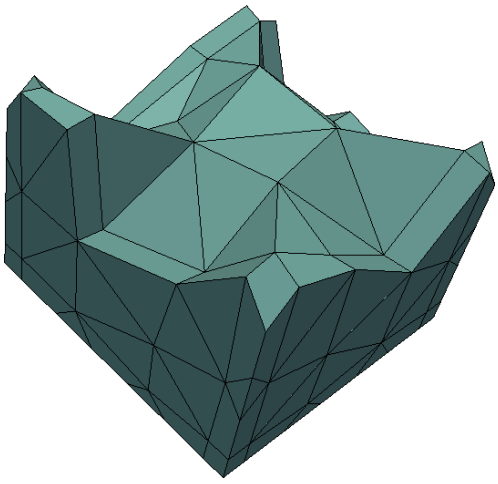

(c) 2nd generation tetrahedral dominant dual mesh, with pentahedral elements forming a boundary layer

Figure 3.15: Formation of boundary layer with cascading mesh generation in 3D

Chapter 4

Polyhedral Mesh Optimization

4.1 Introduction

Following the procedure described in the previous chapter, it is possible to obtain a conforming dual mesh that respects the boundaries of the geometric model, the properties of which are directly and solely dependent on those of the primal mesh. However, it is desired that an analyst should have more control over the mesh generation procedure, in order to obtain meshes of high quality. That being said, one aspect to take into consideration is that mesh validity and quality cannot always be clearly defined but are, rather, concepts that largely depend on the context of use. This is something that applies even for tetrahedral and hexahedral meshes, where validity and quality criteria may vary upon the simulation type and the analysis software. Nevertheless, polyhedra are, in general, considered of not as strict quality criteria, making polyhedral meshes a much more flexible alternative for CFD simulations. In this chapter, an insight to the characteristics that define the quality of a polyhedral mesh is attempted, as well as a description of pre- and post-processing steps that may be applied, in order to optimize the resulting mesh.

4.2 Validity

Depending on the simulation software, polyhedral elements that will satisfy the validity criteria may range from those that provide a non-negative Jacobian at quadrature points, to those that have a strictly positive insphere to circumsphere ratio, with the latter being, for non-simplices, loosely defined. A conservative approach that is likely to satisfy most analysis codes was suggested by Garimella et al., according to which, a polyhedron is considered valid if it passes the star-shaped test [10].

In this method, a measure of convexity is provided, which considers a symmetric decomposition of each polyhedron into tetrahedra. The tetrahedralization takes place around a universal apex at a "central point" of the volume, connected with a base triangle formed by a "central point" of each face and the vertices of the faces, considered in pairs 4.1. In the above procedure, the geometric mean of the vertices of a face may be regarded its center and the same applies for the polyhedral volume. The polyhedron is valid when the signed volume of each of the formed tetrahedra is positive.

In the present work, validity of dual meshes has been specifically resolved according to behavior of the computational tools in hand. The primal tetrahedral meshes, generated by NETGEN mesh generator [18], have, in general, resulted into convex dual polyhedra in the interior, with the occasional presence of slightly non-planar faces. Although this is a factor that may influence convergence and accuracy properties, it has not been an issue, regarding cell validity, for DOLFYN CFD code [3], which has been used as provided within the environment of SOFiSTiK FEA software [1].

However, invalid polyhedra have appeared at reentrant corners of geometric models with sharp concavities. In theses cases, highly concave cells were formed, the centroids of which was located outside the volume of the element, causing the CFD analysis to fail. In order to overcome this restraining effect, an initial solution has been to manually shift the centroids of such elements to a location within their volume. Although this remedy cannot be considered optimal, Dolfyn's validity criteria have been, this way, satisfied and simulations including domains with sharp concavities have been successfully run. Further discussion

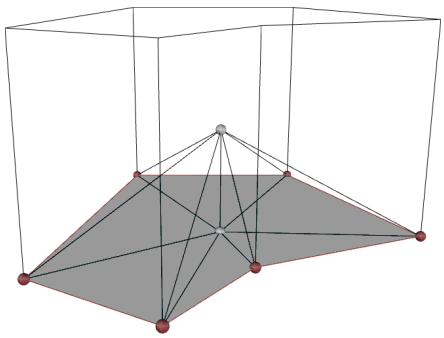

Figure 4.1: Decomposition of polyhedral cell during the star-shaped test

on the effects of this approach on convergence and accuracy is made in (Ch. 5).

4.3 Quality

4.3.1 Selection of Central Points

In the previous chapters, generation of dual meshes has been described using the generic term of *central point*, when referring to a point lying, in general, withing the boundaries of a face or a volume, while, for edges, the unambiguous term *midpoint* is used. These central points define positions of generated dual vertices and their computation is probably the most decisive part of the procedure, having a major impact on the validity and quality of the resulting polyhedra.

A common choice for central points of faces and volumes are their centroids, which are easily computed even for arbitrarily-shaped entities, by performing a decomposition to triangles or tetrahedra, respectively. The advantage of using centroids is that they are always positioned withing their parent-entity, avoiding this way overlapping entities. However, dual faces formed of dual vertices on primal entities' centroids are usually non-planar, introducing local concavities and computationally poor properties to the polyhedra (Fig. 4.2).

For tetrahedral meshes, however, which are the primal meshes of preference in most cases, an alternative "central point" is the triangular faces' and the tetrahedra's circumcenter, as these simplices are always circumscribable. The advantage of using circumcenters is that the resulting dual faces are always planar and, in

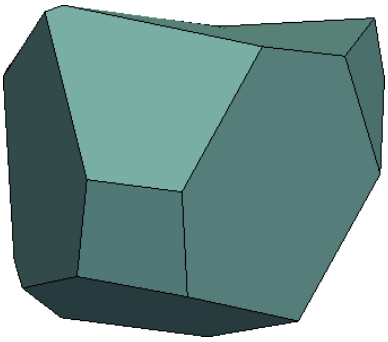

Figure 4.2: Cell concavity due to the presence of non-planar faces

the case that all computed circumcenters are internal, a Voronoi dual mesh is obtained. However, in the case of circumcenters lying outside the boundaries of its parent-entities, invalid dual elements will be generated, overlapping with neighboring entities or leading locally to non-conforming parts of the dual mesh.

It is clear that selecting the optimal "central point" is not always straightforward. An attempt to combine the advantages of both centroids and circumcenters, for tetrahedral primal meshes, is suggested by Garimella et al. [9], where a center should be selected as follows:

- When lying within its parent-entity, the circumcenter of a primal cell shall be preferred
- Otherwise, a point along the line connecting the centroid and the circumcenter shall be used, which is internal and as close as possible to the circumcenter.

With this approach, a valid dual mesh is guaranteed, minimizing the effect of non planar faces within the mesh structure. However, it may result to many of the computed "central points" being positioned very close or on the boundaries of their parent-entity, possibly coinciding with "central points" of neighboring entities that also fall in the same category and forming dual edges of very short length, or even degenerate. Although this not necessarily problematic, in many cases undesired effects are introduced, depending on the analysis, such as very small time steps in simulations [10] or even uncertainties with respect to geometric computations. Such a case occurs while sorting dual vertices counterclockwise, in order to positively define the orientation of dual faces. When the

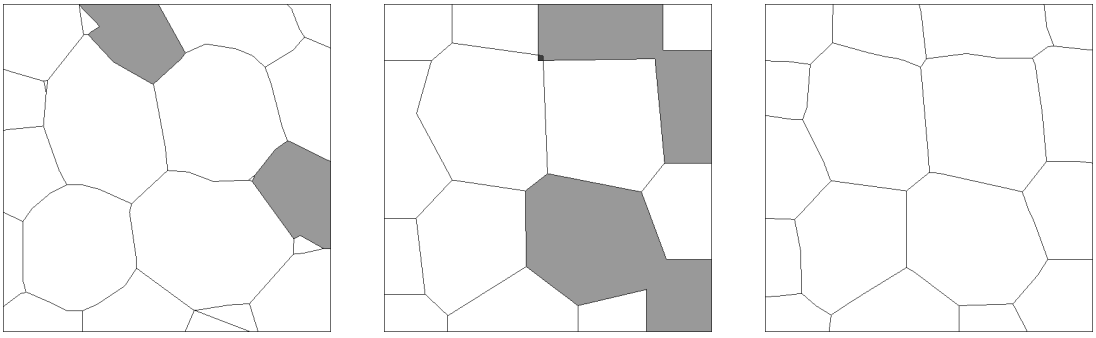

(a) Section of dual cells considering primal cells' centroids – Presence of non-planar faces and concavities

(b) Section of dual cells considering primal cells' circumcenters – Presence of invalid, merged or overlapping elements

(c) Section of dual cells considering a combination of primal cells' centroids and circumcenters

Figure 4.3: Sections of the interior of 3D meshes generated considering different primal cell centers

vertices to be sorted lie very close to each other and given the fact that the rotation center is not exactly positioned on the centroid of the dual face that is about to be generated, the sorting algorithms may fail in returning the correct order of the dual vertices. For the above reasons, it is, hence, necessary that the resulting mesh undergoes a post-processing step, to collapse out very small edges.

In order to avoid the presence of such edges in advance, a minimum distance from the primal cell boundary is suggested to be kept, which will enhance the reliability of the underlying geometric algorithms during mesh generation. This distance may vary according to the quality of the parent-entity. The quality measure of inradius to circumradius ratio may serve as a factor to assure a minimum distance from a primal entity's boundary, that a central point is allowed to be positioned. The following further suggestion is then made to those of Garimella et al. [10]:

- When the circumcenter lies outside the parent-entity's boundaries, the minimum distance from the intersecting boundary, along the centroid-circumcenter line, that a "central point" is allowed to be located, is equal to (1 - ρ) times the length of the centroid-intersection line segment (Fig. 4.4c).

Considering a vector with its origin at the centroid, the above can be expressed as (Eq. 4.1):

$$\overrightarrow{C_dC} = \frac{\overrightarrow{C_dC_r}}{\| \overrightarrow{C_dC_r} \|} \cdot min \begin{cases} \| \overrightarrow{C_dC_r} \| \\ \rho_s \| \overrightarrow{C_dI} \| , \quad \rho_s \in [0,1] \end{cases} \tag{4.1}$$

where ρ_s is a reduction factor which depends on the cell quality , C_d the centroid, C_r the circumcenter, I the aforementioned intersection and C is the internal point where the dual vertex will be located. The common simplices' shape measure that considers the inradius - circumradius ratio [14] has been found to serve well for this purpose (Eq. 4.2).

$$\rho_{tr} = \frac{2R_{in}}{R_{circ}}, \quad \rho_{tet} = \frac{3R_{in}}{R_{circ}} \tag{4.2}$$

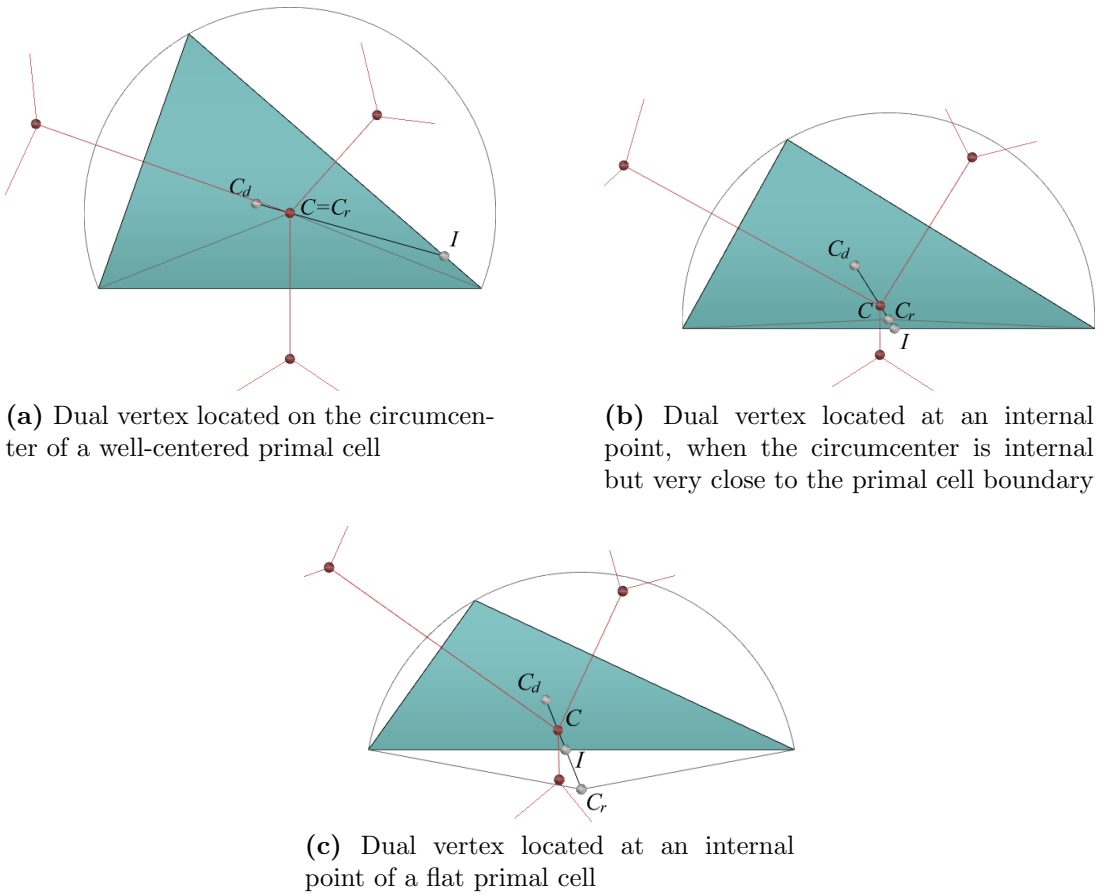

(a) Dual vertex located on the circumcenter of a well-centered primal cell

(b) Dual vertex located at an internal point, when the circumcenter is internal but very close to the primal cell boundary

(c) Dual vertex located at an internal point of a flat primal cell

Figure 4.4: Location of dual vertices for various cases of primal cell quality

The impact of this additional criterion for selecting "central points" has a minor impact on the shape of the resulting polyhedra, improving the polyhedra's angles at this regions but increasing slightly the non-planar effect of those dual faces whose vertices have been affected. The algorithmic stability, however, of the overall dual mesh generation is significantly improved.

4.3.2 Untangling and Smoothing

Given the difficulty to establish unique criteria to measure the quality of polyhedra, several suggestions are encountered in literature, regarding the optimization of polyhedral meshes. A notable effort has been done by Vartziotis and Himpel, wherein the gradient flow of the mean volume of the tetrahedra, formed by decomposing polyhedral elements, is considered [33, 34].

In a more algorithmic-centric approach, improvements for a polygonal surface mesh have been discussed in the past [9], while Dyadechko et al. provide a method for minimizing a global objective function, which considers the sum of a condition number introduced for the corners of polyhedral elements [5]. In this effort, the mesh vertices are repositioned in a minimalistic way, eliminating ill-shaped elements, while keeping the mesh as close as possible to the original one. In the near future, research on a multi-objective optimization is expected, in an attempt to improve the planarity of polyhedral faces [10].

Chapter 5

Validation and Conclusions

5.1 Introduction

The polyhedral mesh generator that has been implemented, has served, apart from the proof of concept, as a tool for exploring the dominant characteristics of polyhedral meshes within the field of CFD simulation. One thing to consider is the fact that mesh generation, itself, is a pre-processing task that may claim a major proportion of the required analysis time. Another significant aspect is the influence of the mesh on the numerics of the analysis, regarding convergence and accuracy. In the following sections, the use of polyhedral meshes in CFD is evaluated, having in mind the impact of meshing on the overall analysis performance. In order to do so, a number of different study cases have been considered, for each of which a polyhedral mesh has been generated and exported. This has served as a geometry input file for DOLFYN CFD code [3], as is provided within the environment of SOFiSTiK FEA software [1].

5.2 Mesh Generation

5.2.1 Memory Requirements

For an indirect polyhedral mesh generation, two data structures, the primal input mesh and the dual mesh, need to be readily accessible at the same time, as the memory allocated for storing the primal mesh can only be released after the polyhedral mesh generation has been completed. It is, thus, of special interest to investigate the overall demand of physical memory required during a dual mesh generation, which involves both coupled data structures.

To this end, a benchmark test has been set up, including a cube of dimensions $1, m \times 1, m \times 1m$, which is initially meshed with tetrahedra. The selected meshing parameters during the primal mesh generation are such that the obtained tetrahedral meshes are of approximately 10, 20, 30, 40, 50 and 60 thousand elements. Following, a polyhedral mesh generation takes place and, until it is complete, the two data structures live simultaneously in the computing system's memory.

Before looking into the memory demands of the overall mesh generation, it is interesting to note the relation between the entities of the two counterparts. As described in chapter 3, one dual cell is formed around every primal vertex, resulting into a one-to-one correspondence between the two. For the rest types of mesh entities, the precise number of dual entities depends on the criteria considered at the boundaries, that indicate the significant primal entities which will result in their contribution to forming a dual entity. That being said, the majority of the primal mesh entities lie in the interior of the domain, where a one-to-one correspondence exists between primal cells and dual vertices, primal faces and dual edges, and primal edges and dual faces.

For the six benchmark cases, the amount of entities per type is summarized in the following table (Tab. 5.1), reflecting the relationships between primal and dual mesh entities as described before. Being able to precisely estimate the amount per type of dual entities, coupled to corresponding primal entities, including those lie on the boundary, can be a useful way to predict and allocate the necessary memory space before the polyhedral mesh generation begins.

Table 5.1: Number of entities for primal and dual meshes

Mesh Type	*Vertices*	*Edges*	*Faces*	*Solids*
Primal	2352	14023	22298	10626
Dual	13002	25868	15219	2352
Primal	4214	26155	42472	20530
Dual	23686	47212	27741	4214
Primal	5959	37771	62014	30201
Dual	33781	67390	39569	5959
Primal	7819	50273	83240	40785
Dual	44505	88826	52141	7819
Primal	10134	63721	104380	50792
Dual	56860	113488	66763	10134
Primal	12158	75532	122632	59257
Dual	68065	135850	79944	12158

In the following graph (Fig. 5.1), the total physical memory occupied by each primal and dual mesh structure is shown, in respect to the mesh size counted in number of cells, tetrahedra or polyhedra. Each point of the dual mesh graph corresponds to a point of the primal mesh's graph, referring to the six benchmark examples that were previously described.

It is shown that physical memory requirements are of linear complexity $O(n)$, with respect to the mesh fineness, both for the primal and dual meshes. Apart from that, there are two main observations that one can make, regarding the demands of memory for the coupled meshes. On the one hand, a dual mesh is significantly more expensive in storage, approximately five times, as in a per cell basis. On the other hand, the number of dual cells is much lower than that of the primal cells, also approximately five times. Combining the two, it is to be noted that the total amount of memory allocated for a primal mesh and that of its dual counterpart is approximately the same, with the dual mesh requiring slightly more memory. This can be explained, due to the increased number of dual entities, as described before, as well as their more complex connectivity that is represented with adjacency tables stored in the mesh data structure.

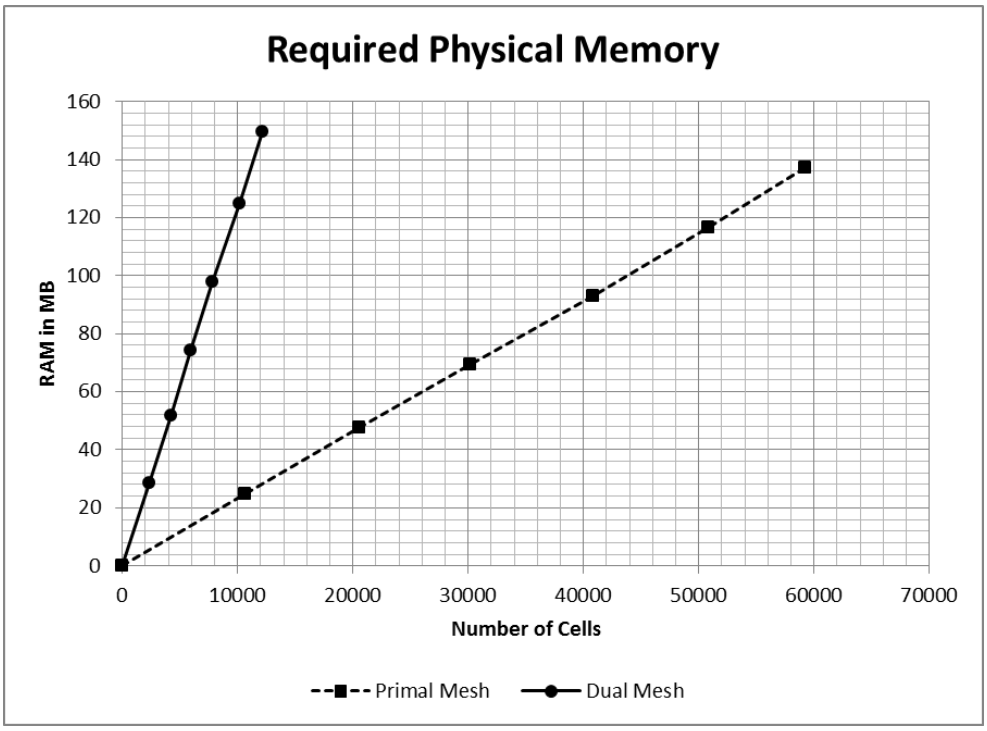

Figure 5.1: Memory requirements for tetrahedral meshes and their polyhedral counterparts

What can be, finally, drawn as a conclusion, regarding storage space requirements in polyhedral mesh generation, is that for a given geometry one should account for a further memory needs, during the mesh generation itself, that is in general within acceptable bounds given the modern computing systems capabilities. In the benchmark examples above, approximately the same amount of physical memory, as that of the tetrahedral input mesh, is additionally allocated for the dual mesh. However, after the polyhedral mesh generation is complete, the memory occupied by the primal mesh may be released and the system's resources are free to be used otherwise.

5.2.2 Performance

Figure (Fig. 5.2) shows how mesh generation time is related to the mesh size, for primal as well as dual meshes. The graphs refer to the same geometry of a unit cube, which was meshed primarily with tetrahedra, using increasing fineness, and their counterpart polyhedral dual meshes. Therefore, the marked points on

each graph are, in an ordered manner, coupled. As an example, a primal mesh of approximately 30k tetrahedra, generated in 27.5s, resulted in a dual mesh of approximately 6k polyhedra, generated in 4.5s.

Polyhedral meshes, as obtained by an indirect method, have shown a satisfactory profile in performance, during the stage of mesh generation. In both primal and dual meshes, it can noticed that the required time increases linearly with respect to the number of elements of the resulting mesh, yielding a linear complexity $O(n)$. Furthermore, the slopes of the two linear graphs are approximately the same, which can be interpreted as an identical ratio of required time per volume element for the two counterpart meshes.

An interesting observation, though, is that the size of a dual mesh is roughly $\frac{1}{5}$th the size of the corresponding primal input, as is the ratio of primal generators vertices to primal cells. This means that polyhedral mesh generation requires approximately $\frac{1}{5}$th of the time of the primal direct mesh generation as well. However, it should not be neglected the fact that dual mesh generation, as part of an analysis procedure, is performed additionally to the primal mesh generation, which constitutes a prerequisite.

5.3 CFD Simulation

The purpose of polyhedral mesh generation, within this study, is to investigate the impact that polyhedral meshes have on computational fluid dynamics, as compared to other, more commonly used, types of meshes. To this end, two analysis cases have been chosen, in order to obtain a first estimation of the accuracy of CFD using polyhedral meshes, as compared to the standard practice of using tetrahedral ones. The 3D domains are selected such that they can be meshed with hexahedra, as well, in order to obtain a comparison of polyhedral meshes with what is considered to be the optimum choice.

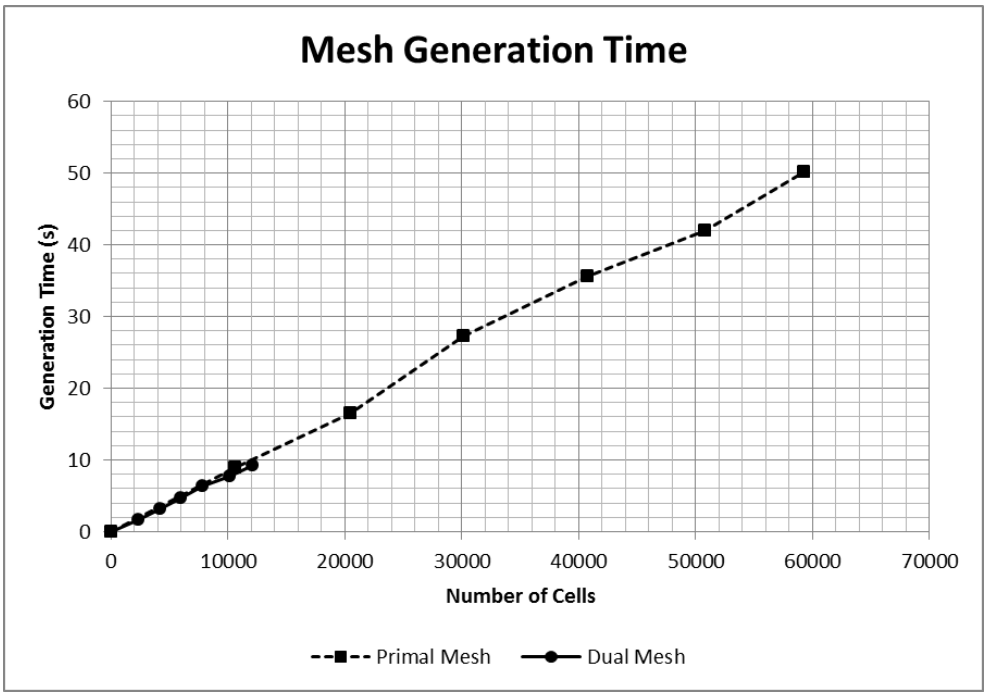

Figure 5.2: Polyhedral mesh generation time in comparison with corresponding primal mesh generation

5.3.1 Laminar Flow Through Cube

In this case study, air flows through a unit volume (Fig. 5.3) with a laminar flow of velocity:

$$U_x = 1.0m/s, U_y = 0.0m/s, U_z = 0.0m/s$$

The volume is meshed with two directly comparable ways: with a hexahedral mesh and with a polyhedral mesh of approximately the same number of cells. Additionally, the tetrahedral primal mesh that was used in order to generate the polyhedral one, is considered as well (Fig. 5.4a – 5.4b). This allows for a comparison between primal and dual meshes, rather than uncoupled tetrahedral and polyhedral meshes or tetrahedral and hexahedral ones. During the analysis, the residuum of U_x is monitored with respect to the number of iteration steps.

What is made clear in graph (Fig. 5.5) is that using the tetrahedral primal mesh, the analysis is unable to converge to the level of the desired tolerance. On

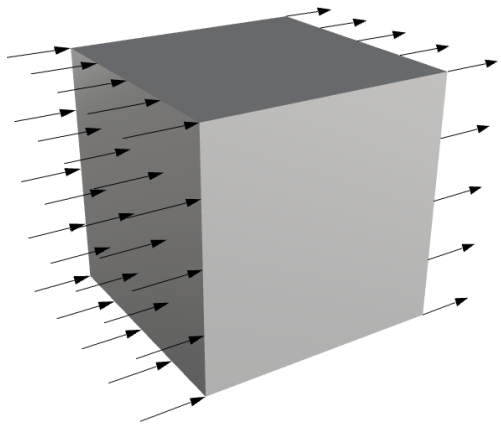

Figure 5.3: Unit cube with laminar flow along a main axis

the other hand, the hexahedral mesh shows a satisfactory analysis progression, approaching to convergence after approximately 60 iterations and stabilizing at approximately 80 iterations. Finally, the polyhedral dual mesh reaches a convergence status at approximately 80 iterations as well.

An interesting remark is that when using polyhedra, while progression towards convergence is noticeably slower than when using hexahedra, a much more stable analysis profile is achieved, with fewer numerical oscillations, mainly concentrated at the beginning of the analysis. This can be explained by the fact that, despite the structured hexahedral mesh lacking any geometrically poor quality elements, the connectivity of polyhedral elements with their neighboring cells is significantly higher, allowing for fluxes of any direction to be accounted for during the finite volume analysis. On the other hand, out of the 26 neighboring cells enclosing an internal hexahedron, 6 of them share a common face with it, allowing only fluxes along the three main directions to be considered.

Finally, considering the convergence progression of the tetrahedral mesh, as well, table (Tab. 5.2) shows the number of iterations that are required in order for the three types of meshes to conclude to the same level of convergence, dictated by the minimum residuum an analysis with tetrahedra can conclude to.

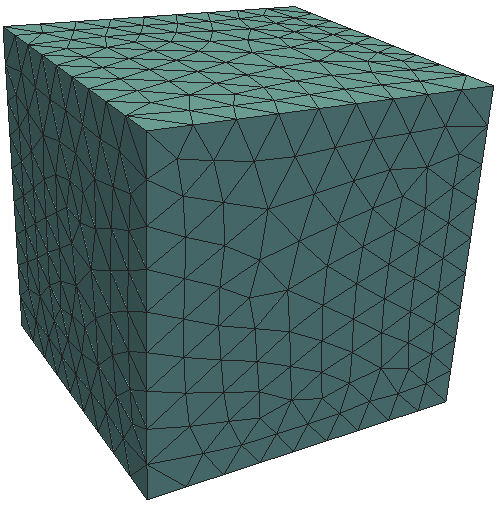

(a) Primal tetrahedral mesh

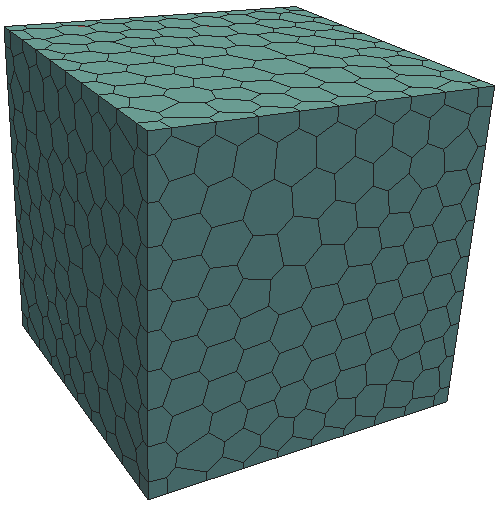

(b) Dual polyhedral mesh

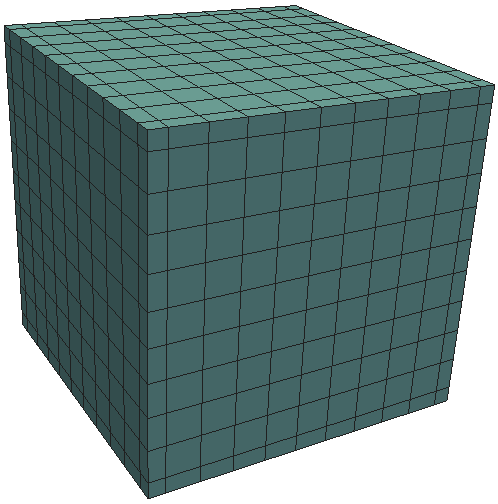

(c) Reference hexahedral mesh

Figure 5.4: Tetrahedral, polyhedral and hexahedral meshing of the 3D domain

Table 5.2: Iterations needed to achieve the same level of convergence

Mesh Type	*Number of Cells*	*Iterations*
Tetrahedral	6168	229
Polyhedral	1336	28
Hexahedral	1331	24

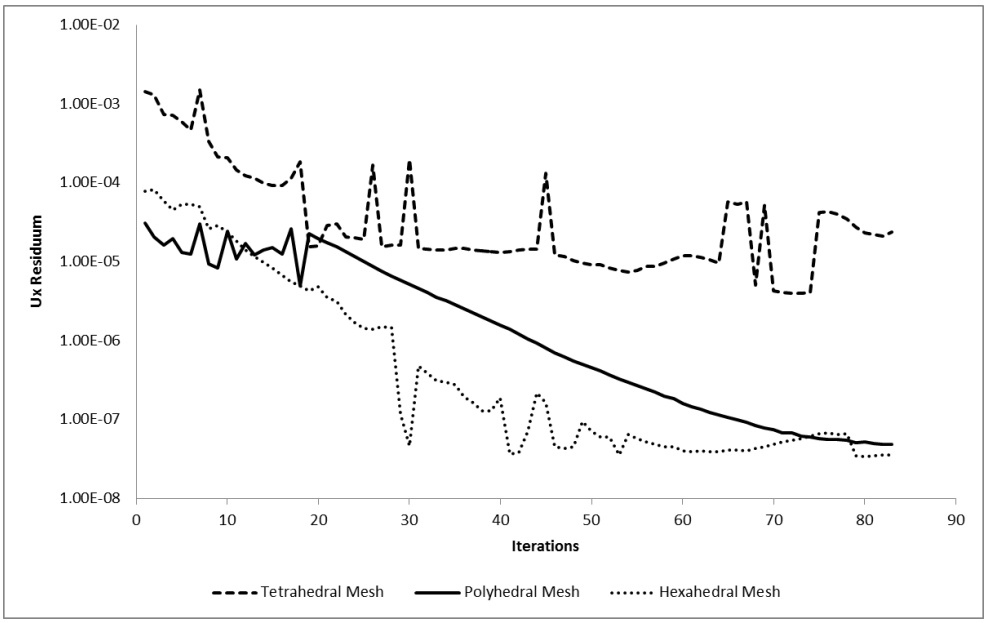

Figure 5.5: Polyhedral mesh generation time in comparison with corresponding primal mesh generation

5.3.2 Laminar Flow Around Cylindrical Object

Another simulation of more complex properties is performed, in the scope of evaluating the use of polyhedral meshes in CFD. The analysis examines the formation of a von Kármán vortex street within a laminar flow, due to the presence of a cylindrical object. The configuration of the analysis is set up according to the specifications of a series of simulations, performed by Sato and Kobayashi [26], that serves as a reference study.

A narrow channel, of dimensions $100 \cdot 10^{-3}m \times 50 \cdot 10^{-3}m$, is formed, with a cylindrical object of diameter $d = 8 \cdot 10^{-3}m$ located in the middle of the channel's width, at $\frac{1}{4}th$ of its length (Fig. 5.6). The fluid is assumed to be water at room temperature, $T = 293K$, with density $\rho = 998.204\frac{(kg)}{m^3}$ and coefficient of viscosity $\mu = 1.002 \cdot 10^{-3}Pa \cdot sec$. A Reynolds number $Re = 195$ is considered, which corresponds to an inflow velocity $U = 24.5 \cdot 10^{-3}\frac{m}{s}$, given by (Eq. 5.1),

$$U = \frac{\mu Re}{\rho L} \tag{5.1}$$

, where L is the characteristic length, which in the case of a flow around a cylindrical object is considered equal to the object's diameter. Additionally, a zero pressure is applied to the outflow boundary and, finally, a non slip condition is assumed on the surface of the cylinder, while a free-slip condition is considered on lateral boundaries.

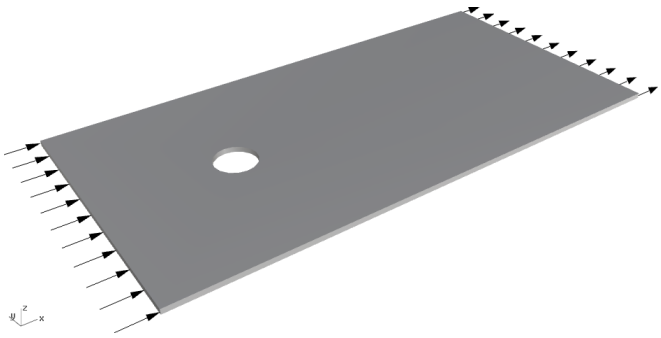

Figure 5.6: Narrow channel with cylindrical object, with laminar longitudinal flow

In the reference study, a structured hexahedral mesh has been used, using elements of thickness $t = 1 \cdot 10^{-3} m$, in order to simulate different cases of flow properties [26]. Herein, the flow characteristics are kept constant, while 6 polyhedral meshes of increasing density are used for the analysis, ranging from approximately 15k (Fig. 5.7b) cells to 65k (Fig. 5.7c). To compare with, a hexahedral mesh of approximately 65k elements is also created, by extruding a 2D unstructured quadrilateral mesh over a thickness t (Fig. 5.7a). Finally, a boundary layer has not been considered in any of the analysis cases.

The simulation is performed within the spectrum of $60 < Re < 200$, which allows the formation of a von Kármán vortex street, due to the presence of the cylindrical object, but avoids the interference with other turbulent phenomena, due to a high Reynolds number [26]. In (Fig. 5.8a), the resulting streamlines of the flow, according to the reference study, are shown. Additionally, a contour plot of the velocity vector is depicted in (Fig. 5.8b), as obtained by the analysis case using the hexahedral mesh of (Fig. 5.7a).

Using progressively finer polyhedral meshes, a set of simulations for the same CFD problem configuration are performed. The corresponding contour plots of the velocity vector are depicted in (Fig. 5.9a – 5.9f). It is shown that the coarser polyhedral meshes of 15k and 25k cells are not able to properly capture the von Kármán vortices formed at this scale. A better approximation comes with

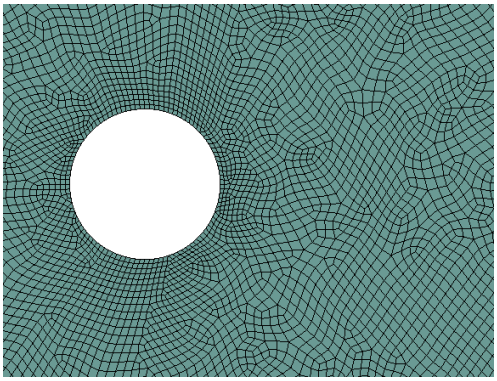

(a) Hexahedral mesh – Cells ≈ 65k

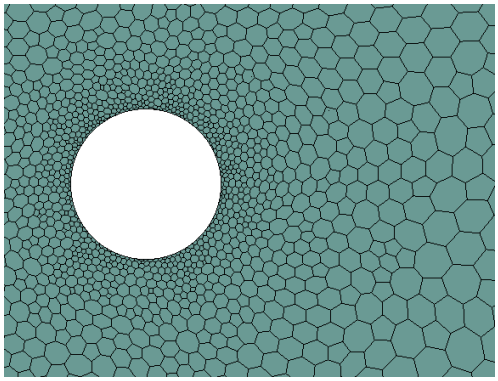

(b) Polyhedral mesh – Cells ≈ 15k

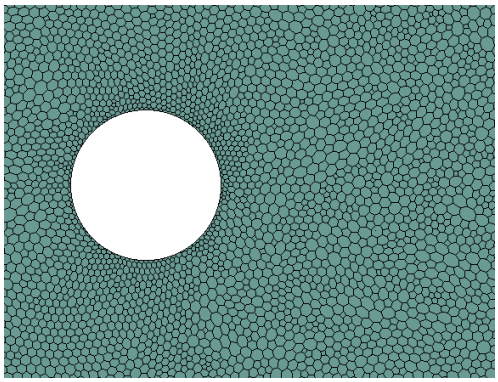

(c) Polyhedral mesh – Cells ≈ 65k

Figure 5.7: Details of mesh cases around the cylindrical object

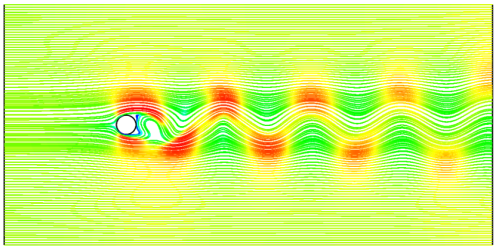

(a) Flow streamlines as presented in the reference study [26]

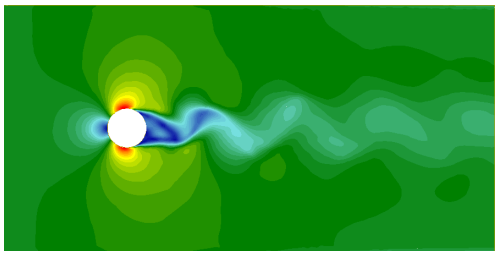

(b) Contour plot of the velocity vector obtained using the hexahedral mesh

Figure 5.8: Reference results

the meshes of 35k and 45k polyhedra, while, for those of 55k and 65k cells, the simulation accuracy, as related to the mesh refinement, seems to have reached the maximum possible. Finally, an analysis case, using a tetrahedral mesh of comparable size, has not been made possible. As shown in (Sec. 5.3.1) and other

studies [21, 28], this would have required a mesh refinement of more than 5 times tetrahedral elements than the number of polyhedra.

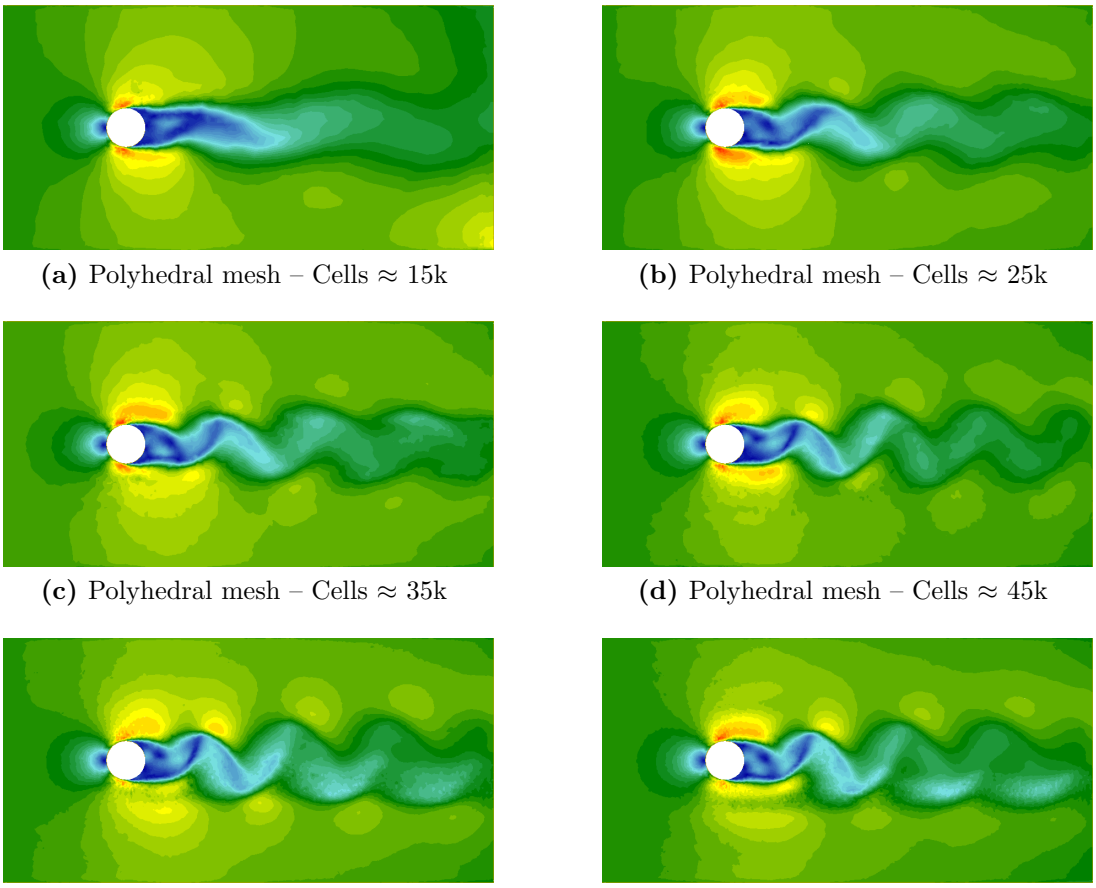

(a) Polyhedral mesh – Cells ≈ 15k

(b) Polyhedral mesh – Cells ≈ 25k

(c) Polyhedral mesh – Cells ≈ 35k

(d) Polyhedral mesh – Cells ≈ 45k

(e) Polyhedral mesh – Cells ≈ 55k

(f) Polyhedral mesh – Cells ≈ 65k

Figure 5.9: Contour plots of the velocity vector for increasing mesh refinement of polyhedral meshes

It should be noted that the contour plots become growingly speckled, as the mesh refinement increases. This can be explained by the fact that an extrapolation of the result positions is made, during post-processing. The computed values, at the centers of the polyhedral cells, are transfered to the vertices of the primal mesh, in order to visualize the results. This causes inconsistencies in the contour plot, that may be overcome by importing the actual result locations in the visualization software, or by applying a bilinear, or other, interpolation of the obtained results, for the positions of the primal vertices.

During the CFD simulation, the component U_x of the flow velocity is monitored

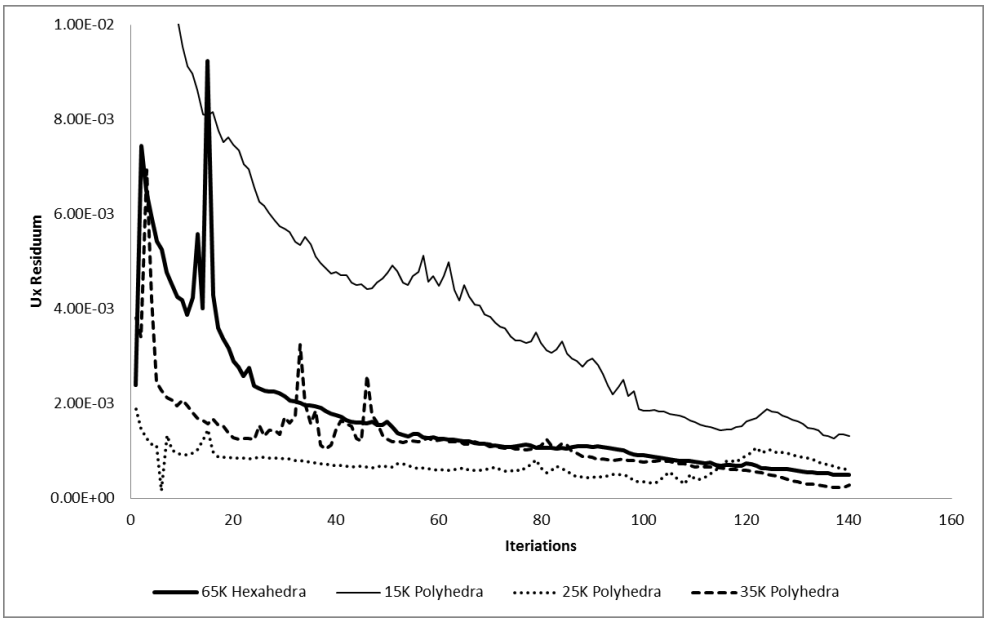

(a) Convergence plots for polyhedral meshes of 15k – 35k elements

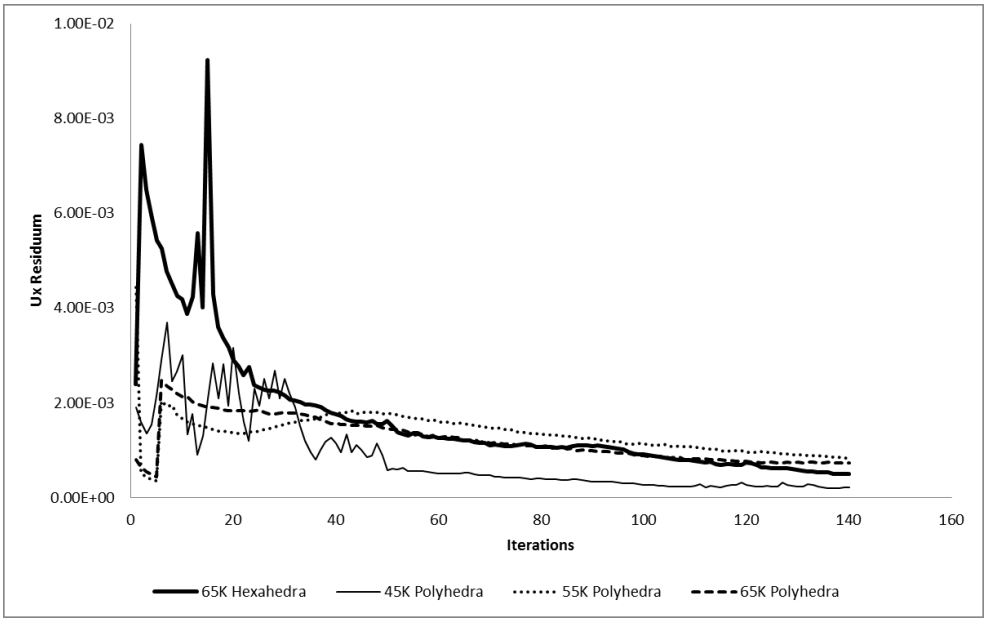

(b) Convergence plots for polyhedral meshes of 45k – 65k elements

Figure 5.10: Comparative convergence plots for polyhedral meshes of increasing refinement, as well as for the hexahedral reference mesh

and, for each polyhedral mesh, a convergence plot for the residual value of U_x is drawn (Fig. 5.10a, 5.10b). In all cases, even for the coarser meshes, the analysis has shown satisfactory accuracy, with velocity in x direction reaching

the expected value of $U_x = 2.45 \cdot 10^{-3} \frac{m}{s}$, according to the problem definition.

For all polyhedral mesh densities, as well as for the reference hexahedral mesh, oscillations are observed at the initial steps of the simulation. With the exception of the coarsest mesh, these gradually smoothen out, as the analysis progresses. However, this has probably not happened for the polyhedral meshes to the extend that had been expected. The total absence of a boundary layer may be an explanation for this behavior. Nevertheless, further investigation on this issue is required, in order to reach a well-established conclusion.

5.4 Conclusions

Polyhedral meshes have attracted the attention of CFD analysts during the past years, as an alternative to the use of tetrahedra, the numerical properties of which are not optimal. In the present work, the use of polyhedra in CFD analysis of complex structures has been studied. Focus has been placed on polyhedral mesh generation methods, with emphasis on the recent work of researchers towards a robust approach, able to produce high quality meshes [10].

To this end, a polyhedral mesh generation code has been developed, following an indirect method based on the principle of duality transforms. Thus, the generation of polyhedral meshes has been made possible. Following, a series of performance and convergence benchmark analysis cases has been performed, in order to evaluate the quality of the resulting meshes. In the present text, an overview of the basic principles on which the development of the mesh generation code has been based is attempted, as well as a discussion over the impact of polyhedral meshes in CFD simulation.

Serving as input, tetrahedral meshes of regular shapes as well as arbitrary geometry have been obtained with the use of NETGEN mesh generator [18], which has proven suitable for the purpose, providing high quality, well-centered primal meshes. The outcome of polyhedral mesh generation has been exported to geometry data files for DOLFYN CFD code [3], as provided within the environment of SOFiSTiK [1]. Additionally, for the purposes of visualization, the creation of VTK files [32] has been made possible, to be viewed with the aid of Paraview

visualization software [35].

The overall complexity of the mesh generation algorithm has proved to be linear, requiring the same amount of computational effort per cell, as needed by the tetrahedral mesh generator that has been used. However, due to the fact that the total number of elements of a polyhedral mesh is about 5 times less than those of its primal, approximately $frac$15th of the corresponding time is needed. It should be emphasized, though, that the computational effort, which is required for polyhedral mesh generation, should be regarded as additional to that of generating a primal mesh.

In terms of storage, a linear complexity has been observed as well, even though the sophisticated topology of polyhedral meshes requires the use of data structures that occupy significantly larger amount of memory per cell, as compared to a tetrahedral mesh. The fact, however, that the number of elements of a polyhedral mesh is far lower than its primal, leads to the two meshes requiring approximately the same amount of storage. This means that, at its peak, the required space in memory becomes two times larger than storing only a tetrahedral mesh. In this area there is certainly room for future improvements, by carefully selecting the mesh representation schemes that are being used, as well as optimizing their implementation.

Regarding the influence of polyhedral meshes on CFD simulation, despite the increase in absolute time required during mesh generation, the performance speed-up during analysis has been observed to more than compensate for the increased pre-processing effort. Polyhedral meshes, that provide the same level of accuracy as tetrahedral ones, are of significantly less elements, which eventually leads to faster and more accurate simulations. Finally, the above observations, regarding performance and accuracy, seem to conform with the conclusions that have been drawn by other studies in the past [21, 23].

With the current implementation, a conforming polyhedral mesh is obtained, respecting the boundaries of the domain as described by the primal mesh. In future efforts, post-processing steps may be applied to the mesh, in order to optimize its topological and geometric properties. Garimella et al. [10] have adequately described a first optimization approach for the geometric properties of polyhedral cell. Focus is currently placed on multi-objective optimization, in

order to reduce the effect of non-planar dual faces. Furthermore, an attempt to address the problem of concave cells at sharp reentrant corners is expected in the near future. These are concepts that would be welcome in a future extension of the present work.

To conclude with, polyhedral elements appear to combine the advantages of hexahedra, in terms of performance and numerical properties, with those of tetrahedra, in terms of flexibility for meshing domains of arbitrary geometry. Additional testing and more detailed benchmark cases are needed, in order to further evaluate the properties of polyhedral meshes, and their influence on CFD analysis, including cases of turbulent flows. The first indications obtained by the present study show a promising future for polyhedra and, given the ongoing research, there may be a time, not far in the future, when polyhedral meshing will be regarded as standard practice within the scope of CFD analysis.

Appendix A

Geometric Computations

A.1 Vertices

Vertices, being the simplest entities in a mesh, participate in most cases simply by their coordinates, which are the only information with geometrical substance stored in the database. Apart from that, the unweighted centroid of a set of vertices is often computed, as a central point during decomposition of polygons and polyhedra, before the weighted centroid of dual faces and solids is known.

$$C_V = \frac{\sum_{i=1}^{n} V_i}{n} \tag{A.1}$$

A.2 Edges

Edges are represented as linear segments defined by two connected vertices, making related geometric computations simple. Their midpoints and length are often required, while they are treated, in many cases, as vectors, knowing their starting and ending vertex.

A.3 Faces

Dual faces are simple, non self-intersecting polygons, defined by an arbitrary number of connected edges. Their shape can be irregular, which demands that concave polygons, while not desirable, are not excluded from geometric algorithms. Furthermore, it cannot be guaranteed that a face, formed by connecting the centers of tetrahedra surrounding a primal edge, is always planar. To be able to handle such arbitrary polygons, their decomposition to simplices is required, commonly known as triangulation.

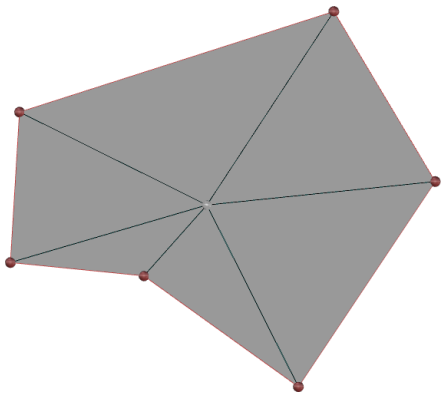

Figure A.1: Face decomposition by triangulation

The normal of polygons is computed by Newell's formula, which is an efficient way to compute face's normals in 3D space [30]. Even in case of non-planar faces, the algorithm is able to produce a vector, representing a uniform normal perpendicular to a "mean" plane, for the set of points that form the polygon. In general, this approach is sufficient, as faces are usually not highly non-planar, and further sophisticated, computationally expensive solutions, such as least square surface fitting, are not necessary.

$$N_{F_x} = \sum_{i=1}^{n} (y_i - y_{i\oplus 1})(z_i + z_{i\oplus 1}) \tag{A.2a}$$

$$N_{F_y} = \sum_{i=1}^{n} (z_i - z_{i\oplus 1})(x_i + x_{i\oplus 1}) \tag{A.2b}$$

$$N_{F_z} = \sum_{i=1}^{n} (x_i - x_{i\oplus 1})(y_i + y_{i\oplus 1}) \tag{A.2c}$$

Computing a polygon's area, involves its decomposition into triangles and the summation of the signed area of each triangle, in order to account for concave shapes. The triangulation takes place using the face's vertices' centroid as a decomposition center, as the polygon's weighted centroid is not yet known. Finally, as the face may not be planar, the computed area is projected to the plane dictated by the previously computed normal. Considering all the above, the area is computed as shown by (Eq. A.3):

$$A_F = \mathbf{N} \cdot \frac{\sum_{i=1}^{n} \overrightarrow{C_V V_i} \times \overrightarrow{C_V V_{i \oplus 1}}}{2} \tag{A.3}$$

Following the same concept, a polygon's centroid is computed by decomposing the face.

$$C_F = \frac{\sum_{i=1}^{n} A_i C_i}{A_F} \tag{A.4}$$

where A_i stands for the signed area and C_i for the centroid of each triangle, formed by two sequential vertices of the faces and the centroid of all of its vertices.

A.4 Solids

Extending the approach followed for geometric computations of polygons, polyhedra are treated by applying a decomposition as well. This type of decomposition is known as tetrahedralization, where a solid is considered as the sum of tetrahedra formed by a central point in its interior, used as an apex, and the triangles of its triangulated faces as tetrahedra bases. As a central point is selected again the centroid C of all vertices that form the solid, while for decomposing the solid's faces, it is now possible to consider each polygonal face's centroid C_F.

The volume of the polyhedron is then computed by:

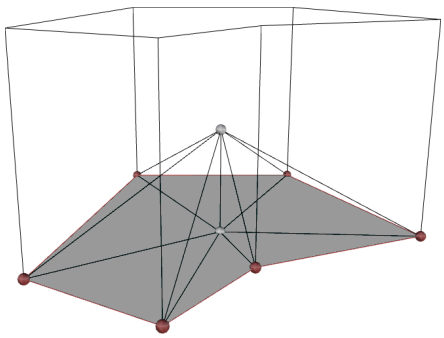

Figure A.2: Polyhedron decomposition by tetrahedralization

$$Vol_S = \frac{\sum_{i=1}^{n} \overrightarrow{CC_F} \cdot (\overrightarrow{CV_i} \times \overrightarrow{CV_{i \oplus 1}})}{6} \tag{A.5}$$

As is the case with the areas of faces, the signed volume of each tetrahedron is computed this way, in order to account for possible concave areas of the solid. Finally, a polyhedron's centroid is computed by:

$$C_S = \frac{\sum_{i=1}^{n} Vol_i C_i}{V_S} \tag{A.6}$$

where V_i stands for the signed volume and C_i for the centroid of each tetrahedron, formed by two sequential vertices of a polygonal face, its centroid the centroid of all of vertices forming the solid.

Appendix B

Source Code

In the attached CD, the source code of the implemented polyhedral mesh generator is included, so that it can be further studied, developed and used as a reference in future work. It should be noted that, as the mesh generator has been specifically developed for creating meshes usable within DOLFYN open source CFD analysis code [3], it cannot be considered a generic tool, suitable for every case where the use of a polyhedral mesh is desired. However, its extension to supporting more CFD simulation software should be possible, by enriching the available mesh export options. Additionally, as the present implementation has been made possible within the environment of the proprietary SOFiSTiK FEA software [1], it cannot be expected that the source code can be usable without any modifications, wherever proprietary dependencies may apply. Despite that, there has been made an effort to keep these dependencies to a minimum level, with the hope that it will prove a useful point of reference for future studies. That being said, the included code is provided as is, without warranty of any kind, and with the permission to study, modify and use for educational purposes.

Contents of the CD:

- Source code of the implemented polyhedral mesh generator
- LaTeX source files of the present document
- The present document in PDF format

List of Figures

List of Tables

Bibliography

[1] SOFiSTiK AG. http://www.sofistik.com.

[2] André Bakker and Elizabeth Marden Marshall. *Computational Fluid Dynamics*, chapter 49, pages 505–515.

[3] DOLFYN Open Source CFD. http://www.dolfyn.net.

[4] Mark de Berg, Otfried Cheong, Marc van Kreveld, and Mark Overmars. *Computational Geometry Algorithms and Applications*. Springer, 2008.

[5] Vadim Dyadechko, Rao V Garimella, and Mikhail J Shashkov. Reference jacobian rezoning strategy for arbitrary lagrangian-eulerian methods on polyhedral grids. In *IMR*, pages 459–470. Citeseer, 2004.

[6] JH Ferziger and M Perić. *Computational Methods for Fluid Dynamics*. Springer, 3 edition, 2002.

[7] R. V. Garimella. Mesh data structure selection for mesh generation and FEA applications. *International Journal of Numerical Methods in Engineering*, 55(4):451–478, October 2002.

[8] R. V. Garimella. Mstk: A flexible infrastructure library for developing mesh-based applications. In *Proceedings of the 13th International Meshing Roundtable, Williamsburg, VA.*, 2004.

[9] R. V. Garimella and M. J. Shashkov. Polygonal surface mesh improvement. *Engineering with Computers*, 20:265–272, 2004.

[10] Rao V. Garimella, Jibum Kim, and Markus Berndt. Polyhedral mesh generation and optimization for non-manifold domains. In Josep Sarrate and

Matthew Staten, editors, *Proceedings of the 22nd International Meshing Roundtable*, pages 313–330. Springer International Publishing, 2014.

[11] Paul-Louis George and Houman Borouchaki. *Delaunay Triangulation and Meshing - Application to Finite Elements*. Editions HERMES, 1998.

[12] J. Gregson, A. Sheffer, and E. Zhang. All-hex mesh generation via volumetric polycube deformation. *Computer Graphics Forum (Special Issue of Symposium on Geometry Processing 2011)*, 30(5):to appear, 2011.

[13] Hrvoje Jasak, Aleksandar Jemcov, and Zeljko Tukovic. Openfoam: A c++ library for complex physics simulations. International Workshop on Coupled Methods in Numerical Dynamics, IUC, Dubrovnik, Croatia, September 2007.

[14] Barry Joe. Shape measures for quadrilaterals, pyramids, wedges, and hexahedra, March 2008.

[15] Michael Kremer, David Bommes, Isaak Lim, and Leif Kobbelt. Advanced automatic hexahedral mesh generation from surface quad meshes. In *Proceedings of the 22nd International Meshing Roundtable*, Berlin, 2013. Springer-Verlag.

[16] Henk Krüs. Dolfyn developers guide, 2010.

[17] H. Ledoux. Computing the 3d voronoi diagram robustly: An easy explanation. In *Voronoi Diagrams in Science and Engineering, 2007. ISVD '07. 4th International Symposium on*, pages 117–129, July 2007.

[18] Netgen. Automatic mesh generator. http://sourceforge.net/projects/netgen-mesher/.

[19] W. Oaks and S. Paoletti. Polyhedral mesh generation. In *Proceedings of the 9th International Meshing Roundtable 2000*, pages 57–66, 2000.

[20] OpenFOAM. The open source computational fluid dynamics toolbox. http://www.openfoam.com/.

[21] M. Perić. Flow simulation using control volumes of arbitrary polyhedral shape. In *ERCOFTAC Bulletin, No. 62*. September 2004.

[22] M. Perić. Simulation of flows in complex geometries: New meshing and solution methods. In *NAFEMS Seminar: Simulation of Complex Flows (CFD) – Application and Trends*, 2004.

[23] M. Perić and S. Ferguson. The advantage of polyhedral meshes. http://www.cd-adapco.com/.

[24] Qhull. http://www.qhull.org/.

[25] E. Ruiz-Gironés. *Automatic Hexahedral Meshing Algorithms: From Structured to Unstructured Meshes.* PhD thesis, Universidad Politécnica de Cataluña, January 2011.

[26] M. Sato and T. Kobayashi. A fundamental study of the flow past a circular cylinder using abaqus/cfd. Mechanical Design & Analysis Corporation.

[27] Joachim Schöberl. Netgen an advancing front 2d/3d-mesh generator based on abstract rules. *Computing and visualization in science*, 1(1):41–52, 1997.

[28] Martin Spiegel, Thomas Redel, Y Jonathan Zhang, Tobias Struffert, Joachim Hornegger, Robert G Grossman, Arnd Doerfler, and Christof Karmonik. Tetrahedral vs. polyhedral mesh size evaluation on flow velocity and wall shear stress for cerebral hemodynamic simulation. *Computer methods in biomechanics and biomedical engineering*, 14(01):9–22, 2011.

[29] STAR-CCM+. http://www.cd-adapco.com/products/star-ccm.

[30] D. Sunday. Fast polygon area and newell normal computation. *Journal of Graphics Tools*, 7(2):9–13, 2002.

[31] TetGen. A quality tetrahedral mesh generator and a 3d delaunay triangulator. http://wias-berlin.de/software/tetgen/.

[32] Visualization Toolkit. http://www.vtk.org/.

[33] D. Vartziotis and B. Himpel. Efficient Mesh Optimization Using the Gradient Flow of the Mean Volume. *ArXiv e-prints*, February 2013.

[34] Dimitris Vartziotis and Benjamin Himpel. Efficient and global optimization-based smoothing methods for mixed-volume meshes. In Josep Sarrate and

Matthew Staten, editors, *Proceedings of the 22nd International Meshing Roundtable*, pages 293–311. Springer International Publishing, 2014.

[35] Paraview Open Source Scientific Visualization. http://www.paraview.org/.

[36] Voro++. http://math.lbl.gov/voro++/.

[37] Dong-Ming Yan, Wenping Wang, Bruno Lévy, and Yang Liu. Efficient computation of 3d clipped voronoi diagram. *Advances in Geometric Modeling and Processing*, pages 269–282, 2010.

[38] Yongjie Zhang, Xinghua Liang, and Guoliang Xu. A robust 2-refinement algorithm in octree and rhombic dodecahedral tree based all-hexahedral mesh generation. In Xiangmin Jiao and Jean-Christophe Weill, editors, *Proceedings of the 21st International Meshing Roundtable*, pages 155–172. Springer Berlin Heidelberg, 2013.